Response to review Reviewer 1
Christner et al., Microbial processes in the weathering crust aquifer of a temperate glacier
Please note pages/lines referenced by the authors are to revised text

1. **Comments from Referee:** "*My main suggestion for improvement is related to the presentation of the sampling procedure in the boreholes, which I think is a crucial part of the study. I am sure most readers would like to have a better visualisation of how samples were obtained by having some photos and/or a schematic figure (either in the main paper or as supplementary information). I have no doubt that the study has captured well the weathering crust microbial processes. The data of microbial composition provides some solid evidence of a different community in the WCA compared to the surface community, and some more information in the methods would help to make this point clear*".

   Author's response: We agree with this suggestion.

   Author's changes in manuscript: A new figure has been included in the revised manuscript (Supplementary Figure 1 in revision) that includes a schematic of the approach we used for sampling and an image of a water sample being retrieved from one of the boreholes.

2. **Comments from Referee:** *"Page 4, line 16 – Please specify how the boreholes were monitored. I think this will also help to clarify the first paragraph of the results section."*

   Author's response: Science personnel were on site daily from approximately 9 AM to 6 PM local time (i.e., during the diurnal peak of surface melt water production). The content of each drained borehole was examined daily (detailed inspection each morning after arriving on site and then periodically through the day). During the 2014 and 2015 sampling periods when it was verified that water was percolating laterally and collecting in the boreholes, each was monitored at no less than hourly intervals when personnel were on site.

   Author's changes in manuscript: Additional information about how the boreholes were monitored has been added to the text (Pg 4, lines 18-22).

3. **Comments from Referee:** *"Page 8, line 18 – please specify the volume of the serum vials."*

   Author's response: The water was collected in 30 mL serum vials

   Author's changes in manuscript: This information has been added to the text (Pg 8, line 23).

4. **Comments from Referee:** *"Last paragraph of page 17 – Maybe it is worthy to mention/reinforce the fact that the sample used for those incubations has a relatively high proportion of Cyanobacteria/plastids. Nevertheless, the cell number increase during the oxygen consumption experiment indicates a strong bottle effect during the incubations. It would be good if this can be further discussed in line with the calculations in the first paragraph of page 18."*

   Author's response: These important points were not sufficiently emphasized in the manuscript.

   Author's changes in manuscript: In the revision, the high abundance of phototrophic taxa inferred in the near-surface samples is referenced directly with respect to the oxygen consumption results

(Pg 17, lines 29-30). We also revised the text to acknowledge that ex situ assays inevitably involve sampling disturbances and may provide conditions that allow microorganisms to reproduce at higher than in situ rates (i.e., the "bottle effect"; Pg 18, lines 9-10).

5. **Comments from Referee:** *"The literature on microbial processes at the very ice surface provides quite often evidence for organic carbon accumulation, which in turn results in the darkening of the ice. Is it possible for the authors to make inferences (based on the incubation experiments and microbial community composition of the WCA) whether the WCA microbial processes could have a role on surface activity (e.g., via recycling of nutrients that become available to surface organisms as the ice ablates exposing WCA communities at the surface)?"*

   Author's response: While we mention how biogeochemical processes on the ice surface may influence those occurring in the WCA, the reverse scenario was not mentioned.

   Author's changes in manuscript: A sentence has been added to the concluding paragraph (Pg 20, lines 26-27) stating the possibility that biomass turnover in the WCA may also mineralize and mobilize nutrients that fertilize biological activities on the ice surface.

Response to review Reviewer 2
Christner et al., Microbial processes in the weathering crust aquifer of a temperate glacier
Please note pages/lines referenced by the authors are to revised text

1. **Comments from Referee:** *"The more significant observation is that the use of borehole thermistor data from 15m to 45m seems to be somewhat inappropriate. This is outside the zone of interest, and the discussion of these results alludes to weaknesses in both the thermistor data itself and the modelled ice temperature, at least to make confidence in both aspects rather clouded. This detracts and confuses the paper, and takes the reader into areas that simply add little to the focus of the paper. Recommendation would be to simply use the modelled surface temperature profiles to 15m as a proxy for the temperature conditions. The other thermistors lie outside this, so while useful to test the broader scale applicability of the thermal model, the deeper measurement points can not really be used to validate the near-surface model, particularly with the uncertainties discussed, and so seem to be simply adding data unnecessarily (nor essential) to the paper. Suggest removal of all information on the uncertain borehole data. Simplify this to the use of the model as a proxy estimate for the surface conditions. Discussion can then allude to the need to better characterise the thermal behaviour of the WCA, and instrument the uppermost few metres, including adding the potential influence of snow cover on thermal regime over the full annual cycle."*

   Author's response: We thank the reviewer for thinking carefully about the relationship between modeled and observed temperatures. We have removed the 45 m temperature record as it does seem to detract from the main points we make in the paper. Moreover, it appears that we need to do a better job at explaining in the manuscript the take-away messages from both of these approaches. The output from our heat diffusion-production model is used in this manuscript to illustrate how subsurface temperatures and water content would evolve if the near-surface part of a glacier would behave as a homogeneous ice mass subjected to realistic surface temperature and radiation forcings. The model output is clearly shown in our figure (Fig. 1A) before it is used to compare model predictions with field temperature observations (Fig. 1C). Hence, readers interested in predictions of our idealized model can easily understand them before moving onto the part where we compare modeled and observed ice temperatures.

   The field observations of temperatures at different depth demonstrate that, in reality, our study site is heterogeneous and allows processes other than heat diffusion and penetration of sunlight to impact ice temperatures. Our field temperature data suggest that the processes perturbing temperature distribution in a heterogeneous way involve vertical transport and refreezing of water (to explain observations of ice temperatures warmer than predicted by the model at a given depth) as well as flow of cold air through fractures and/or conduits (to explain observations of ice temperatures colder than predicted by the model at a given depth).

   The mismatch between the observed and modeled temperatures does not represent noise that detracts from the focus of this paper but does represent by itself an insightful scientific finding. Basically, our model output represents a hypothesis and our field observations allow us to test this hypothesis. In this case we reject the hypothesis of homogeneous subsurface and speculate which features of the real system can explain the mismatch between model and observations. Future work by our team, or other researchers, may enable modeling of the effects of vertical water and air transport through fractures and conduits. However, at the present time we simply do not have sufficient data to treat these effects in a realistic, quantitative manner. Similarly, we do not have the data that would justify inclusion of a snow cover into our model. Generally, such a snow cover

should produce two competing effects: (1) it will thermally insulate the underlying ice hindering its winter cooling, but (2) it will also hinder internal solar heating of the ice itself until the winter snow cover is completely melted. The two effects may largely cancel each other and should not have first-order impacts on the key results of our model.

Author's changes in manuscript: We removed the 45m temperature record from Figure 1C and changed the discussion of these results (Pg 12, lines 1-15).

2. **Comments from Referee:** *"P2 Opening paragraph, seems to slightly confuse the goal and focus of the study, and could be seen as rather weak and less targeted than perhaps might be achieved. Recommend revisiting and reworking. Now, the concept of glacier surfaces as an ecosystem (e.g. Hodson et al., 2008; Stibal et al., 2012, Nature Geoscience; Hotaling et al., 2017, Environmental Microbiology) is well-accepted, and the references particularly to firn storage rather distract from the core topic here which is the shallow near-surface ice in the ablation zone. Preference might be to keep the study's focus clear from the outset to better guide the reader. Perhaps better to consider Cooper et al. (2018, Cryosphere) and Smith et al. (2017, PNAS) who focus on water storage in bare ice in Greenland, or delayed runoff in mountain glacier settings (Munro, 2011, Hydrological Processes). Consider opening with need to understand the ice surface as a locus of biological activity, relevant with recognition of water storage and delay. This would better guide the reader into the material that follows."*

   Author's response: These are excellent suggestions.

   Author's changes in manuscript: The discussion of firn aquifers has been eliminated and replaced with text describing how the weathering crust influences the timing and magnitude of meltwater delivery to supraglacial, subglacial, and proglacial systems (Pg 2, lines 7-10).

3. **Comments from Referee:** *"L25: Perhaps reference to earlier LaChapelle (1950s) work on this, and Munro's (1990) examination of subsurface melting would be appropriate to evidence knowledge of this phenomenon. Similarly, Muller and Keeler (1969) were the first to use "weathering crust" specifically for glacier ice, although others used ablation rind, honeycomb ice, ablation crust etc. (see earlier discussion texts regarding glacier ice structure) – perhaps revise citation position to highlight and better evidence this and source of the terminology."*

   Author's response: We thank the reviewer for providing information on the earliest observations that shaped understanding on the structure, formation, and properties of the weathering crust.

   Author's changes in manuscript: The LaChapelle (1959) and Munro (1990) papers are cited in the revision and the text has been edited to unambiguously attribute the term "weathering crust" to Müller and Keeler (1969) (Pg 2, lines 26-28).

4. **Comments from Referee:** *"P3 L2: Particularly for temperate glaciers – could be emphasised, given this is one aspect of novelty here. Note, here, given Larson's (1977, 1978) studies on water balance and meltwater storage in the nearsurface of an Alaskan glacier, it is surprising these references are absent, and they could be helpful for defining or better justifying the depth range of WCA zone examined and sampled here. See earlier comment regarding maintaining clear focus in the opening sections. See also Fountain and Walder's (1998) comments on this ice 'zone'."*

Author's response: That there have been no studies of weathering crusts in temperate glaciers is a point worth emphasizing. The intention of the paragraphs' final sentence is to stress the dearth of information on biogeochemical processes in the near-surface aquifers of any glacier. As such, we believe that a description of water balance and storage for other Alaskan glaciers moves this discussion off point.

Author's changes in manuscript: The final paragraph in this sentence has been edited to mention that no data has been available on the weathering crust ecosystems of temperature glaciers (Pg 3, lines 2-5).

5. **Comments from Referee:** *"P4 L14: The authors hoefully should be aware of Stevens et al. (2018, Hydrological Processes) as well as Cooper et al. (2018, Cryosphere) – perhaps here, and/or elsewhere, recognition could be given to work examining porosity and permeability of the WCA. This is a current topic, and updates to sources cited could be included to keep the paper contemporary."*

   Author's response: Agreed but such a discussion is not appropriate in the methods section.

   Author's changes in manuscript: The porosity and permeability observations of Cooper et al. and Stevens et al. on the WCA are now referenced in the introduction (Pg 2, lines 7-9) and discussed on Pg 16, lines 26-29.

6. **Comments from Referee:** *"P5 L23: Perhaps missed something in this section, but the "water content" aspect isn't perhaps as clear as could be effected. This section seems to describe temperature in detail, but does not quite give a sufficiently direct indication of water content calculations, especially if calculated for the model domain rather than the porous layer itself. Suggest clarification for readers less familiar with thermal models for ease of accessibility, given water volume is later reported in figures."*

   Author's response: We thank the referee for catching the fact that our methods section did not include sufficiently detailed explanation of our approach towards calculating internal melt water fraction.

   Author's changes in manuscript: We added a few sentences that explain how internal water content is calculated in the model (Pg 6, lines 16-19).

7. **Comments from Referee:** *"L5 L24: For the WCA, typically only a few m, the use of a 45 m borehole seems to be excessive and rather misaligned with the zone of interest (see earlier comment). Similarly the model of 100 m seems to lie outside the region of observations. Note misalignment of information between the 45 m borehole and the 20 m of thermal data presented, update caption to reflect this – and perhaps reflecting earlier suggestion of reducing the use of less certain thermal data. While use of deeper temperature records to seek to validate the thermal model is admirable, there seem to be significant uncertainties both in the model and the thermistor data that render this approach equivocal and conjectural. See comment above, which may help here."*

   Author's response: As mentioned above, we think it is important to keep some of the comparison of observed temperatures to modeled temperatures. We have followed referee's suggestion and deleted the 45 m record, which was the most different from its simulated equivalent. However, we do think that it is important to retain the comparison between the temperatures at the other depths

as they underline the point that the upper part of the glacier is highly heterogeneous in reality and enables vertical advection of heat, water, and microbial matter. We see no benefit in limiting the discussion to just the results of simulations.

Author's changes in manuscript: We have deleted the 45m temperature record from Figure 1C and changed the results section accordingly (Pg 12, lines 1-15).

8. **Comments from Referee:** *"P16 L20: Fountain and Walder (1998, Reviews Geophysics) discuss the WCA and Irvine-Fynn et al. (2011) phrase this as a "perched aquifer". Also see Stevens et al. (2018, Hydrological Processes), Cooper et al. (2018, Cryosphere), and Smith et al. (2017, PNAS)."*

   Author's response: We are aware of prior classification of the WCA as a perched aquifer but are confused about the intention of this comment.

   Author's changes in manuscript: None.

9. **Comments from Referee:** *"L27: Consider revising as the WCA may be shallow (see LaChapelle's earlier work), and while lower density (by volume) ice may exist at the surface, typically the water table lies below this. See Muller and Keeler's (1969) conceptual diagram of this, and as evidenced by water depths in cryoconite holes. It would therefore be unlikely that ice would show a 50% liquid water by volume, rather this might be the very weathered surface ice, from which melt drains to the denser near-surface. Similarly, the Antarctic comparison seems to understate the thermal conditions both at surface and subsurface, which would influence WCA development. Recommend adjusting the wording here to reflect this and making comparisons more relatable."*

   Author's response: We agree with these suggestions.

   Author's changes in manuscript: The sentence discussing the unlikely possibility of water contents as high as 50% has been eliminated and we have edited the comparison to Antarctic weathering crusts by pointing out that the ice is much colder and that the penetrating radiation is mostly used to warm the ice rather than melt it (Pg 16 lines 25-29).

10. **Comments from Referee:** *"P18 L4: given the temperature model excludes snow cover (see Methods description), is the 7.5 months realistic, and does this tally with in situ snow cover, which itself will affect WCA development and closure? Perhaps revise values here to reflect this, or caveat that this neglects the influence of snow on the WCA – a process yet to be reported."*

    Author's response: This is an important point that we now discuss. We do not have the data to explicitly treat the problem so we discuss how inclusion of snow cover could change our results.

    Author's changes in manuscript: We have included a discussion of this on Pg 18 (lines 4-9).

11. **Comments from Referee:** *"P20 L12: This section becomes more conjectural and loses focus on content of paper. Suggest revising conclusion to reflect the data and relationships shown. Nothing here directly reports on biological influence on the albedo of glaciers. Rather, identification of a functional microbial environment on a temperate glacier – which supports ideas and aspects revealed in Arctic and ice-sheet settings – is important. Note, there are perhaps two 'definitions' of "biological darkening": one potentially introduced in Irvine-Fynn et al. (2012, Environmental*

Microbiology) referring to microbe-mineral retention; and secondly, the more recent phrasing used when referring to the 'bio-albedo' and apparent darkening of some ice surfaces by active biomass (e.g. van den Broeke et al, 2017, Current Climate Change Reports) which was termed "biotic acceleration of glacier melt" (Koshima et al., 1993, IAHS). However, the processes underlying these definitions are subtly different. Importantly, none of the references cited specifically use the phrase "biological darkening". Much of the bioalbedo is related to ice surface algae, not necessarily the same community as that in the WCA. Please use quotations correctly, and recommend retaining focus on actual data and findings of the paper rather than seeking to link to other topic areas."

Author's response: We agree with this suggestion.

Author's changes in manuscript: The text referring to biological darkening has been removed and the conclusion section has been edited to focus the data presented (Pg 20-21, lines 25-29, 1-4).

12. **Comments from Referee:** *"P2 L20: Scott et al. (2010, Ann Glaciology) show microbial nutrient turnover in supraglacial streams, which may be relevant here."*

    Author's response: Agreed.

    Author's changes in manuscript: The observations of Scott et al. are now discussed in this section (Pg 2 lines 17-20).

13. **Comments from Referee:** *"L21: Please use multiplication not the letter 'x'. Noted elsewhere throughout (e.g. P6 L14)."*

    Author's response: Agreed.

    Author's changes in manuscript: The multiplication symbol now replaces "x" here and throughout the revised text.

14. **Comments from Referee:** *"P6 L8: Check journal style, but perhaps revise unit to ◦C."*

    Author's response: Agreed.

    Author's changes in manuscript: The text has been revised to present the value as "mm $^{o}C^{-1}$ d^{-1}".

15. **Comments from Referee:** *"P7 L3: Confirm KPAR is K in equation."*

    Author's response: Yes, KPAR is K in the equation and the confusion is understandable.

    Author's changes in manuscript: The text has been revised to make KPAR/K unambiguous (Pg 7 lines 11-12).

16. **Comments from Referee:** *"P9 L9: Check journal style for unit / constant here."*

    Author's response: None

Author's changes in manuscript: The "x" has been replaced with the multiplication symbol.

17. **Comments from Referee:** *"P10 L30: Define rs and rp here, as used elsewhere in Results section."*

    Author's response: None

    Author's changes in manuscript: Designations for the Pearson's and Spearman's correlation coefficients now appear on Pg 11 lines 3-4.

18. **Comments from Referee:** *"P11: Results, please check stylistics as throughout there are contrasting uses (or absences) of '0' before decimal points. A pet peeve is some journals/publishers that have removed zeros from quantities – whether numeric measurements or statistical values."*

    Author's response: By convention, the zero before the decimal point of correlation coefficients are typically omitted. However, we are not married to this convention.

    Author's changes in manuscript: A zero had been added before the decimal for correlation coefficients reported throughout the manuscript.

19. **Comments from Referee:** *"P11 L17: revise and condense. Near-surface is unlikely, by definition, to be 45 m at depth."*

    Author's response: See our response to comment #1. We have removed the 45 m temperature record.

    Author's changes in manuscript: This section has been renamed as "Physical conditions" (Pg 11, line 20).

20. **Comments from Referee:** *"P12 L15: Slight repetition from Methods. Suggest simply presenting equation in methods including citation, and referring to this here with result."*

    Author's response: Agreed

    Author's changes in manuscript: The text has been edited to eliminate redundancy with the methods (Pg 12 line 19).

21. **Comments from Referee:** *"P12 L19: See Larson (1970s) references to support this depth of WCA or photic zone, if thermally still below zero. Consider further in discussion."*

    Author's response: This sounds like a relevant paper to read and potentially cite; however, we are not sure of the study that the reviewer is referring to.

    Author's changes in manuscript: None

22. **Comments from Referee:** *"P13 L12: see earlier comment re. definition of correlation coefficients. Condense."*

    Author's response: We have made this change (see response above).

Author's changes in manuscript: A zero had been added before the decimal for correlation coefficients reported throughout the manuscript.

23. **Comments from Referee:** *"P14: Check style for p-values. Italic elsewhere. See also P19."*

    Author's response: Some p-values were not italicized in the initial version and we could not find guidelines for presenting p-values in TC.

    Author's changes in manuscript: All p-values reported in the manuscript have been italicized for consistency.

24. **Comments from Referee:** *"P17 L11: unit consistency, elsewhere L/m2, later here, use of superscript negatives for 'per'. Recommend check and edit."*

    Author's response: The conversion to superscript units makes this sentence quite awkward, i.e., "200 L of liquid water m^{-2} of glacier surface…". Hence, we have kept the original text.

    Author's changes in manuscript: Figure 1 has been edited so units are presented as L m^{-2} and W m^{-2}.

25. **Comments from Referee:** *"P17 L13: Repetition of P12 L11-20, and immediately above. Revise, avoid repetition."*

    Author's response: The results discussed on Pg 12 describe the maximum depths in the ice that could support photosynthesis based on maximum PAR values. In contrast, the discussion on Pg 17 emphasizes the shallowest depths in the WCA that could theoretically support photosynthesis under the minimum PAR flux values of civil twilight.

    Author's changes in manuscript: None

26. **Comments from Referee:** *"P18: L7: Again, perhaps see Stevens et al. (2018). L18: useful to consider Xiang et al. (2009, FEMS Microbiology Ecology) as this is not altogether a new concept and has been discussed in the literature. L30: "emergence of ice in the actively melting ablation area" might be a stronger phrasing."*

    Author's response: L7: The revision cites Stevens et al. (2018) elsewhere but since this study focused on water (and not microbial) transport, it is not as relevant to this discussion as the work of Irvine-Fynn et al. (2012), which measured concentrations and fluxes of cells from a supraglacial catchment. L18: We realize that ice-immured microbes released into meltwater is not a new or previously unrecognized concept. Our main point is to stress that the differences observed in the biogeochemical and molecular data at depths >2 m are consistent with the microbial assemblages that were directly released by melting from englacial ice. L30: We agree with this excellent suggestion.

    Author's changes in manuscript: The text on Pg 19 line 5 has been edited as recommended.

27. **Comments from Referee:** *"P19 L9: Unclear why access to bed is relevant here, suggest simply noting the fracture networks present in temperate ice may provide an explanation for near-surface to*

englacial linkage might be sufficient, particularly for emergent ice in the ablation area. L31: use "more than" rather than > here."

Author's response: Agreed

Author's changes in manuscript: Both suggested changes have been made (Pg 19 lines 15-16; Pg 20, line 8).

Microbial processes in the weathering crust aquifer of a temperate glacier

Brent C. Christner[1,2*], Heather F. Lavender[2], Christina L. Davis[1], Erin E. Oliver[2‡], Sarah U. Neuhaus[3], Krista F. Myers[4], Birgit Hagedorn[5], Slawek M. Tulaczyk[3], Peter T. Doran[4], William C. Stone[6]

[1]University of Florida, Department of Microbiology and Cell Science, Biodiversity Institute, Gainesville, FL 32611 USA
[2]Louisiana State University, Department of Biological Sciences, Baton Rouge, LA 70803 USA
[3]University of California Santa Cruz, Department of Earth and Planetary Sciences, Santa Cruz, CA 95064 USA
[4]Louisiana State University, Department of Geology and Geophysics, Baton Rouge, LA 70803 USA
[5]Sustainable Earth Research LLC, Anchorage, AK 99508 USA
[6]Stone Aerospace, Del Valle, TX 78617 USA
[‡]Current address: San Diego State University, Department of Biology, San Diego, CA 92182 USA

Correspondence to: Brent C. Christner (xner@ufl.edu)

Abstract. Incident solar radiation absorbed within the ablation zone of glaciers generates a shallow perched aquifer and seasonal ice-bound microbial habitat. During the melt seasons of 2014 and 2015, borehole investigations were used to examine the physical, geochemical, and microbiological properties in the near-surface ice and aquifer of the temperate Matanuska Glacier (southcentral Alaska). Based on temperature, solar forcing, and ice optical properties, the dissipation of shortwave radiation promoted internal melting and the formation of a weathering crust with a maximum depth of ~2 m. Boreholes into the weathering crust provided access to water percolating through the porous ice. The water had low ion concentrations (4-12 μS cm^{-1}), was aerobic (12 mg O_2 L^{-1}), contained 200 to 8,300 cells mL^{-1}, and harbored growing populations with estimated in situ generation times of 11 to 14 days. During the melt season, the upper 2 m of ice experienced at least 3% of the surface photosynthetically active radiation flux and possessed a fractional water content as high as 10%. Photosynthetic subsistence of biogeochemical reactions in the weathering crust ecosystem was supported by ex situ metabolic experiments and the presence of phototrophic taxa (cyanobacteria, golden and green algae) in the aquifer samples. Melt water durations of ~7.5 months coupled with the growth estimates imply biomass may increase by four orders-of-magnitude each year. Our results provide insight on how seasonal dynamics affect habitability of near-surface ice and microbial processes in a portion of the glacial biome poised to expand in extent with increasing global temperature and ablation season duration.

1 Introduction

Annual melt cycles generate water on the surfaces of glaciers and ice sheets that is transported through a sinuous network of channels to the margin as supraglacial runoff or glacier bed via crevasses and moulins to be discharged subglacially (Smith et al., 2008; Chu, 2014). Meltwater can also be temporarily stored on the surface in cryoconite holes (Hodson et al., 2008; Edwards and Cameron, 2017), supraglacial lakes (Fitzpatrick et al., 2014; Langley et al., 2016), and near-surface aquifers within the ice (Hoffman et al., 2014; Karlstrom et al., 2014; Cook et al., 2016). The low-density, highly porous surface ice prevalent in ablation zones serve as reservoirs for meltwater, affecting the timing and magnitude of its delivery to supraglacial, subglacial, and proglacial systems (Munro 2011; Smith et al., 2017; Cooper et al., 2018; Stevens et al. 2018). As such, ice mass loss driven by warming temperatures has motivated numerous efforts to understand how surface meltwater production, storage, and hydrology will affect future sea level rise (e.g., Bamber and Aspinall, 2013) and subglacial hydrological processes that influence ice velocity and ice sheet thinning (Zwally et al., 2002; Sole et al., 2011).

Glacial meltwater production also provides aquatic environments that are suitable for supporting microbial communities and promoting active biogeochemical cycling on glacier surfaces (Hodson et al., 2008; Edwards and Cameron, 2017). Conditions in certain supraglacial environments even fall within the tolerances of cold-adapted multicellular organisms and invertebrate populations have been documented in a number of cryoconite ecosystems (Zawierucha et al., 2015). The uptake of nutrients and dissolved organic carbon in fast flowing supraglacial streams demonstrates the effect of microbial activity on meltwater composition and implies that higher degrees of biogeochemical processing are possible with longer hydrologic retention times (Scott et al. 2010). Visual discoloration of snow and ice surfaces due to blooms of cyanobacteria and algae are commonly observed (Hopes et al., 2017), and in regions with standing water (e.g., cryoconite holes), photosynthetic rates can be sufficient for positive net community productivity (Anesio et al., 2009; Hodson et al., 2013). An important consequence of microbial growth and pigment production is darkening of the ice surface and albedo reduction (Yallop et al., 2012; Stibal et al., 2017; Tedstone et al., 2017); a critical parameter governing surface melting (Gardner and Sharp, 2010).

In the ablation zone, the absorption of shortwave radiation within the ice promotes internal melting and density reduction (LaChapelle 1959; Munro 1990), forming a highly porous veneer on the glacier surface termed the weathering crust (Müller and Keeler, 1969). Flow paths through the weathering crust's saturated water table link segments of the supraglacial hydrological system, transporting microbes and nutrients via subsurface flow (Irvine-Fynn et al., 2012; Hoffman et al., 2014; Karlstrom et al., 2014; Cook et al., 2016). The

availability of photosynthetically active radiation (PAR) in the near-surface aquifer may support phototrophic metabolism (Hodson et al., 2013; Irvine-Fynn and Edwards, 2014), allowing the development of microbial communities in the glacial weathering crust during the melt season. The weathering crust aquifer (WCA) is presumed to be an important component of the hydrological and biogeochemical budget for cold-based glaciers (Irvine-Fynn et al., 2012; Cook et al., 2016; Rassner et al., 2016), but no data have been available to assess microbial activities and biogeochemical transformations in temperate ice systems.

This study examined physical, geochemical, and microbiological properties in the weathering crust of the temperate Matanuska Glacier (located in the Chugach Mountains of southcentral Alaska) to gain information on the nature of the near-surface aquatic ecosystem it supports during the ablation season. Comparison of water percolating through the weathering crust to the surface ice melt revealed unique geochemical features and the enrichment of certain microbial taxa in the WCA, supporting that it may possess distinct biogeochemical processes and species within the supraglacial environment. Sufficient PAR fluxes exist with depth in the ice for photosynthetic activity, and the WCA samples contained growing cell populations and phototrophic taxa. We use these biogeochemical data and modeling results to speculate on how microbial processes in the weathering crust are likely affected by seasonal variability of temperature, light, and water availability.

2 Methods

2.1 Site description

The Matanuska Glacier is a ~48 km valley glacier with an upper accumulation zone at an elevation of ~3500 masl and the terminus is at ~500 masl; its width ranges from ~ 3 km near the equilibrium line to ~5 km along the terminus (Arcone et al., 1995). The measurements and samples analyzed in this study were collected in the vicinity of a research site established on the western lateral margin in the ablation zone of the glacier (61 42' 9.3"N, 147 37' 23.2"W) during June to July of 2014 and 2015, approximately 8 km from the glacier terminus. Science and technical operations were performed on the ice surface and in portable shelters that contained various scientific equipment, including a 61 × 31 cm laminar flow hood (Fungi Perfecti LLC, Item no. E-ALFH1). A meltwater stream ~100 m upglacier from the research camp was sampled to provide a measure of the microbial community structure in supraglacial water environments in proximity to the study site.

2.2 Borehole sampling of ice and water

Boreholes were melted into the ice surface using three different approaches. First, water heated using a diesel-fueled water heater (Pressure-Pro Inc.) was circulated through a tapered aluminum melt head (10 or 30 cm in diameter; 30 cm in length) that was attached to a standard garden hose and manually guided while descending through the ice. Secondly, an electrically-heated copper melt head of 10 cm was used to create boreholes of up to 8.5 m depth. The electrothermal heater was powered with a portable 2.5 kW generator, with the primary front heater reaching up to 2 kW power output and enabling ice penetration rates of 1-2 m per hour. Finally, 25 to 30 cm boreholes were generated with a laser-powered ice-penetrating cryobot that heated the water and used on-vehicle hot water jets to melt the ice and control its direction and rate of descent (Stone et al., 2014, 2018). In June 2014, four −30 cm diameter boreholes (BH1-3 and BH-5; 4 to 30 m in depth) and one −10 cm diameter borehole (BH4; 4 m in depth) were used to sample ice and water in the WCA (Supplementary Table 1). The same location on the glacier was revisited during June to July 2015, and two-30 cm diameter boreholes (BH6 and BH7; 1.4-15.4 m in depth) and three-10 cm diameter boreholes (BH8-10; 4 to 5 m in depth) were sampled (Supplementary Table 1).

In the 30 cm diameter boreholes, particulates in large volumes of meltwater (up to 404 L) were size fractionated (i.e., particulate fractions >3 μm, <3 to >0.8 μm, and <0.8 to >0.2 μm) and concentrated in situ on 142 mm Supor PES membranes (Pall) using a McLane Large Volume Water Transfer System (WTS-LV; Christner et al., 2014). Water in the boreholes was also sampled by lowering clean silicone tubing into the borehole and using a peristaltic pump to deliver the water to the surface. To determine if the ice was porous and active water flow was occurring through the weathering crust, water was drained from several of the boreholes and monitored daily to assure that melt water was not entering directly from the surface. Two of the drained boreholes refilled with water that percolated laterally from the WCA (BH4 and BH10; Supplementary Table 1), and each was subsequently monitored at approximately hourly intervals when personnel were on site (typically 0900 to 1800 local time). The borehole water was retrieved at the surface using sterilized tubing and a peristaltic pump or by lowering clean acid-washed HDPE bottles into the borehole using nylon paracord (Supplementary Fig. 1).

Meltwater samples from discrete ice depth intervals were obtained using a customized water sampler and filtration system that was integrated as a scientific payload on the cryobot (Clark et al., 2017; Stone et al., 2018). Operation of the cryobot requires a water-filled cavity; therefore, the 30 cm aluminum melt head was used to create a ~1 m pilot hole, the meltwater generated was replaced with an equal volume from a supraglacial

stream, and this water was continually circulated through a 0.2 μm filter for ~1 h to reduce the number of microorganisms in the priming water. Stainless steel SwageLok fittings and tubing from the melt head were connected to a peristaltic pump, which was used to pump water into sterile 120 mL capacity sampling bags (Labtainer™ BioProcess Container, cat. No. SH30658.12; 10 total per mission) or through 90 mm Supor PES filters with a 0.2 μm pore size (5 total per mission). The sampling bags had duel ports: one for filling through a sanitary check valve and one for overflow, which was controlled by a sanitary pressure relief valve. The filters were housed within a Savillex filter holder made of PFA fluoropolymer and sealed with Ultem clamps. During water or filtration sampling, the cryobot was operated in "passive" mode (i.e., the hot water jets were not used and heat transfer was directed only to the melt head of the vehicle; Clark et al., 2017), which melted the ice at a rate of ~1 L min^{-1}. To prevent inadvertent collection of bulk borehole water, the sampling pumps were operated at a rate of 56 mL min^{-1} (i.e., ~6% of the rate of melt water generation). Based on the rate of descent and collection, each water sample of 120 mL represented the melt generated from a depth horizon of approximately 1.6 cm in the ice.

2.3 Conductivity, pH, and chemical composition of the water samples

Electrical conductivity and pH of the water samples were measured using a multi-parameter PCSTest probe (Oakton Instruments, Vernon Hills, IL).

The concentration of major ions and trace elements in the water samples were analyzed using inductively coupled plasma mass spectrometry with a reaction cell for cations (ICP RC-MS, Agilent 7500c) and ion chromatograph (Dionex ICS 5000+) for anions. For ICP RC-MS analysis, samples were acidified to 1% HNO_3 v/v and analyzed for 28 elements. Elements prone to interferences (e.g. Ca^{2+} and As^{3+}) were analyzed using H_2 and He as the reaction gas. Quantification was performed using seven external calibration standards ranging from 0.1 to 100 ppb. Drift correction was achieved by online addition of 10 ppb of a four element internal standard mix (Li(7), Y, Ce, and Bi). An IonPac AS15 2x250 mm column was used for anion separation using 38 mM KOH as eluent and ASRS 300 zero reagent suppressor. The sample injection volume was 10 μL and quantification was performed using five external calibration standards ranging from 0 ppm to 10 ppm. Calibration verification standards and blanks were run every 10^{th} analysis for anions and cations. The NIST SRM 1643d was used to verify cation calibration and a secondary anion standard (Anion II Std Dionex) was used to check anion calibration. Samples that exceeded the calibration by 120% were diluted and reanalyzed. Nitrite was not analyzed due to overlap with bicarbonate in the chromatogram. The mass balance deficit between anions and cations was used to determine bicarbonate concentrations.

2.4 Ice temperature and meltwater content

Vertical gradients of temperature in the ice surface were measured over two months during the summer of 2015 by deploying a sensor string into a borehole with thermistor sensors placed at every 10 m along the string and collecting data at hourly intervals. The thermistors were calibrated under controlled conditions and had an accuracy of ca. 0.1 ^{o}C.

A one-dimensional finite-difference model utilizing the explicit Euler central difference method was used to calculate ice temperatures within 100 m of the surface at 0.25 m vertical intervals and with hourly time step. Since Matanuska Glacier is temperate, the lower boundary condition was set to the pressure-melting point while the surface condition was driven using the 2 m-air temperature and the surface downwelling shortwave flux in air. Because these quantities are not available from nearby weather stations, the European Centre for Medium-Range Weather Forecasts ERA Interim reanalysis data for the 0.75 by 0.75 degree cell containing this region of the Matanuska Glacier for the period between the beginning of 2014 and the end of 2016 was used (Fig. 1B; Dee et al., 2011). Air temperature is taken to be equal to the surface temperature at the top of the model domain when the former is negative but is set to the melting point of ice when air temperature is positive. When the latter is the case, the surface melt rate was calculated using the Positive-Degree-Day parametrization (van Beusekom et al., 2010) and a melt factor of 5 mm $^{o}C^{-1}$ d^{-1}. The surface melt rate, which typically reaches several cm per day in summer (Ensminger et al., 1999; Reynolds, 2005; Mankoff and Russo, 2013), was treated throughout the 100 m-thick model domain as spatially uniform upward advection. Surface solar radiation downwards from the ERA-interim dataset was used to scale internal heating in the upper, optically translucent part of the glacier following the exponential Lambert Law of light attenuation with e-folding length scale of 0.825 m as constrained by the PAR data (Fig. 2A). When ice is at 0^{o}C and still experiencing internal heating from solar radiation, the additional heat is used to calculate melt water fraction using the latent heat of ice fusion (334,000 J kg^{-1}). Similarly, when wet ice is cooling down, the negative heat budget is used to first freeze the internal meltwater and ice temperature can drop below 0^{o}C only when its internal water content reaches zero. Heat conduction was treated as a diffusive process using a diffusion coefficient of 1.2×10^{-6} m^2 s^{-1}. The model neglects the impact of seasonal snowpack on either the temperature or energy balance of the simulated glacier surface. In winter, such snow pack would slow cooling of underlying glacier ice while in early summer it would hinder light penetration into the glacier near-surface. The entire model domain was initialized as temperate ice and then the calculation cycled through repeats of the 3-year surface forcings until the drift of calculated ice temperatures reached <0.01 ^{o}C over a 3-year cycle.

2.5 Determination of the PAR fluence rate

PAR (400-700 nm) was measured in boreholes using a LI-COR LI-193 Spherical Underwater Quantum Sensor (LI-COR, Inc) and 10 m underwater cable. The stated sensitivity of the LI-193 is typically 7 μA per 1,000 μmol s^{-1} m^{-2} in water. PAR was also measured at the ice surface with a LI-COR quantum sensor mounted on a small board using a leveling device. Both sensors were driven and logged by a LI-COR LI-1400 Data Logger and were calibrated prior to the first field season.

Two types of measurements were made in water-filled boreholes: vertical profiling within a short period of time and overnight measurement at a fixed depth. For profiling, the sensor was deployed in a 10-cm diameter borehole and measurements were taken from 0 to 8.5 m at 0.5 m increments. To mitigate the "borehole effect" caused when measuring transmitted light in a liquid-filled borehole, the sensor was placed 1 m below a 10-15 cm opaque packer (Muni-Ball®, Cherne Industries Inc.) that was inflated at discrete depths to create a light-tight seal. To avoid freezing the packer in the ice during overnight deployments, the sensor was deployed at 3.5 m in a 30 cm diameter borehole and light was blocked from entering with an opaque tarp. Due to the larger distance between blocked light and the sensor, the diel measurement may have been subject to a larger borehole effect than the profile measurement.

The PAR attenuation coefficient was derived as described by Hodson et al. (2013) based on $PAR(Z) = PAR_0 e^{-KZ}$, where Z is the ice depth from the surface in meters, PAR_0 is the surface PAR flux in μmol m^{-2} s^{-1}, and K is the PAR attenuation coefficient.

2.6 Epifluorescence microscopy

The water samples collected for epifluorescence microscopic analysis were immediately fixed by addition of sodium borate-buffered formalin (5% final concentration), stored at ~4°C, and analyzed within 1 month of collection. Cells were concentrated by filtering 10 to 40 mL of sample onto 0.22 μm black Isopore filters (Millipore, cat. no. GTBP02500) and stained for 15 minutes in the dark with SYBR™ Gold (Molecular Probes Inc., cat. no. S-11494) buffered in Tris-borate-EDTA (pH 8.3). The staining solution was pulled through the filter by applying vacuum, the filter was mounted on a microscope slide, and a drop of antifade (0.1% phenylenediamine in a 1:1 ratio of PBS and glycerol) was added to the middle of the filter before applying a coverslip. For each sample, the number of DNA-containing cells in sixty fields of view (FOV) was enumerated using an Olympus BX51 epifluorescence microscope. The cell concentration was estimated by calculating the

average number of cells per FOV, multiplying by the number of FOVs per filter, and dividing by the volume of sample filtered.

2.7 Determination of ATP biomass

Triplicate measurements of ATP were performed on each sample in the field by concentrating the cells in 25 mL of water on a 0.22 μm Millex-GS Syringe Filter (Millipore, cat. no. SLG033SS), followed by passing 0.2 mL of Extractant B/S from the ATP Biomass Kit HS (Biothema Inc., cat. no. 266-112) and collecting the filtrate. For each procedural replicate, one-quarter of the filtrate (50 μL) was added to 400 μL of ATP Reagent HS and luminescence was measured using a 20/20n luminometer (Turner Biosystems, cat. no. E5331). Subsequently, 1 pmol of an ATP standard was added to each sample and luminescence was measured, allowing the relative luminescence units (RLUs) for each measurement to be corrected for possible inhibition of the luciferase enzyme and/or changes of ambient temperature during the course of measurement. The quantity of ATP was determined by generating standard curves (six 10-fold dilutions of 100 nM to 1 pM ATP) that allowed relating RLUs to the ATP concentration.

2.8 Detection of respiring cells via reduction of a tetrozolium salt

An assay with the tetrazolium salt XTT [2,3-Bis(2-methoxy-4-nitro-5- sulfophenyl)-2H-tetrazolium-5- carbox-anilide] was performed in the field to assess cellular respiration activity. The water sample (50 L) was filtered through a 142 mm, 0.22 μm SUPOR filter (Pall) and the retentate was suspended in a volume of filtrate that concentrated material > 0.2 μm in diameter approximately 1500-fold. Aliquots of this suspension (1 mL) were amended with the XTT reagent (XTT Cell Proliferation Assay Kit, Trevigen Cat. No. 4891-025-K) to a final concentration of 330 μM; the electron-coupling agent (phenazine methosulfate) was not included in the assay (see Roslev and King, 1993).

Individual samples in 1.5 mL microcentrifuge tubes were placed in 50 mL conical tubes that were either transparent or covered with black electrical tape (i.e., dark incubation), affixed to a nylon tether, and incubated in the borehole at a depth of 1.5 m below the surface. A packer (Muni-Ball®) was inflated 1 m above the samples to prevent direct light transmittance through the water in the borehole. At designated time points, formazan production was determined in triplicate samples by measuring absorption at 470 nm with an Ocean Optics USB4000-UV-VIS miniature spectrometer.

2.9 Dissolved oxygen concentration and oxygen uptake rates

The concentration of dissolved oxygen was measured using Winkler titration and the Dissolved Oxygen Test Kit (Hanna Instruments, cat. no. HI3810). To determine oxygen uptake rates, samples of the water were dispensed into 30 mL serum vials (Wheaton, cat. no. W223743) and sealed with butyl rubber stoppers while ensuring that no air bubbles were present in the headspace. During transport from the field site and shipment to the laboratory at Louisiana State University, the samples were kept chilled on blue ice and stored in the dark. Two weeks after sample collection, the serum vials were transferred to an environmental chamber, temperature probes were placed directly above the vials, and the samples were incubated at 5°C. All samples were incubated under a continuous illumination of ~270 μmol photons m^2 s^{-1}, with half of the vials covered with aluminum foil for dark incubation. Over the course of 117 days, triplicate measurements of dissolved oxygen concentration and cell abundance were made on the samples. Rates of oxygen uptake and cell growth at 5°C were adjusted to the in situ temperature of 0°C using the Arrhenius equation and an energy of activation of 15,000 cal mol^{-1} (Priscu, 2013).

2.10 DNA extraction, amplification of 16S/18S rRNA gene sequences, and phylogenetic analysis

The filters obtained for nucleic acid extraction were quartered, placed in cryotubes containing a solution of 40 mM EDTA pH 8.0 and 50 mM Tris pH 8.3, and stored chilled in an insulated cooler on the glacier for approximately 1 week. Immediately after return from the field, sucrose was added to the storage buffer (final concentration of 0.73 M), the cryotubes were frozen, and shipped overnight to Louisiana State University on blue ice. The samples were stored in a laboratory freezer at -80°C until analyzed.

To extract DNA from the filters, a sterile scalpel was used to cut the filter into small pieces to enhance yield during bead beating. Sterile forceps were used to transfer the filter pieces to bead beating tubes. The storage buffer remaining in the cryotubes was centrifuged at 16,000 × g for 10 min to pellet any particulates remaining in the storage buffer, and this material was added with the filter to the bead beating tubes. DNA was extracted from the samples using the Power Water DNA Isolation Kit (MO BIO Laboratories, Inc.) with the following modifications of the manufacturer's instructions. First, some of the extracted filters were separated into two bead beating tubes for the initial steps of the protocol, and subsequently, the supernatants were combined on a single spin filter. Second, the samples were incubated at 65° C for 10 min after adding the lysis buffer followed by bead beating in a Mini-Beadbeater-16 (Bio Spec Products Inc.) at 3450 oscillations min^{-1} for 4 to 5 min. Lastly, the filter was washed with an additional volume of Solution PW1, vortexed, centrifuged, and

the supernatants were pooled. The genomic DNA was suspended in 10 mM Tris buffer, quantified by absorbance at A_{260} using a Nanodrop (Thermo Fisher Scientific) or with a Qubit fluorometer (dsDNA HS Assay Kit, Thermo Fisher Scientific), and stored at -20°C. Three blank filters were included in the DNA extraction protocol to serve as procedural controls for the molecular analysis.

A portion of the 16S rRNA gene (V4 region) was amplified from the extracted genomic DNA samples using the oligonucleotide primers 515F and 806R (Caporaso et al., 2012). Each 25 or 50 μL PCR reaction contained 0.1 to 6 ng of genomic DNA, 3 mM $MgCl_2$, 1X Gold buffer, 0.2 mM dNTP's, 0.2 μM of each primer, and 2.5 U of AmpliTaq Gold DNA polymerase LD (Invitrogen). The amplification conditions included an incubation at 95°C for 8 to 10 min followed by 35 to 45 cycles of denaturation at 94°C for 30 s, annealing at 50°C for 30 s, and extension at 72°C for 45 s. A final extension was performed at 72°C for 5 min. The amplicons were evaluated by electrophoresis through a 1% agarose gel, purified using the MoBio UltraClean PCR Clean-Up Kit, quantified with Qubit fluorometry, and 240 ng of each amplicon was pooled. Paired-end sequencing was performed using the Illumina MiSeq platform (RTSF Genomics Core at Michigan State University and ICBR NextGen DNA Sequencing Core at University of Florida).

Barcodes and adapters were removed using Trimmomatic (v0.36; Bolger et al., 2014) and the amplicon sequences were processed using mothur (Schloss et al., 2009). Paired end sequence reads of the V4 region were assembled into contigs and quality filtered using the following default parameters: maximum sequence length of 275, minimum quality score of 25, and maximum ambiguous bases of 0. Sequences were aligned with the mothur compatible SILVA database (v128). Chimeric sequences were removed using the VSEARCH algorithm within mothur. The mothur-formatted Ribosomal Database Project (RDP) training set (v16) was used to assign all sequences with ≥97% similarity to an operational taxonomic unit (OTU). Singletons and OTUs in the procedural controls were removed before data normalization. To assess community diversity and richness of the samples, the OTU abundance data were normalized (9,151 sequences); Good's estimator of coverage and Simpson's diversity index were calculated in mothur. Abundant OTUs were defined as having a relative abundance of ≥ 0.1% of the total sequences. Non-metric multidimensional scaling (NMDS) plots were calculated within mothur and visualized in R (v.3.4.1; R Core Team, 2017).

A portion of the 18S rRNA gene (V4 and V5 regions) was amplified using genomic DNA isolated from sample BH10d and the universal eukaryal primers F566 and R1200 (Hadziavdic et al., 2014). PCR reactions of 25 μL contained 2.8 ng of genomic DNA, 1X Taq buffer A, 0.5 mM dNTP's, 0.5 μM of each primer, and 1.25 U of Taq polymerase (Fisher BioScience). The amplification protocol started with a 3 min incubation at 95°C, followed by 35 cycles of denaturation at 95°C for 30 s, annealing at 60°C for 45 s, and extension at 72°C for 1

min. A final extension was done at 72°C for 10 min. Gel electrophoresis through a 1% agarose gel was used to evaluate amplicon size and clone libraries were constructed with the TOPO TA Cloning Kit for Sequencing (Invitrogen) according to the manufacturer's instructions. Individual clones (25) were cultured in Miller LB media containing 50 μg mL^{-1} of ampicillin and plasmid DNA was purified using the PureLink Quick Plasmid Miniprep Kit (Invitrogen). Plasmid DNA was quantified with a Nanodrop 2000c (Thermo Scientific) and 50-150 ng of each was used to bi-directionally sequence each insert by Sanger sequencing (Eton Bioscience, Inc.).

Phylogenetic tree construction was conducted by aligning the query sequences based on secondary structure to their nearest neighbors using SINA Alignment Services (Pruesse et al., 2012). The sequence alignment was trimmed using MEGA7 and a phylogenetic tree was created with the maximum likelihood method (Kumar et al., 2016). Bootstrap values were calculated in MEGA7 based on Felsenstein's method and 1000 replicates.

2.11 Statistical analysis

The assumption of normality was evaluated using the Shapiro-Wilk test. The strength of linear and montonic correlations between geochemical and microbiological variables was assessed by evaluating Pearson's (r_p) and Spearman's (r_s) correlation coefficients, respectively. Student's t-distribution test was applied to determine the probability of significant differences between variables ($\alpha \leq 0.05$). Statistical differences between the microbial communities were evaluated using analysis of molecular variance (AMOVA) in mothur (Schloss et al., 2009).

3 Results

3.1 Evidence for a porous weathering crust and near-surface aquifer system

During the first eleven days of field work in June 2014, there was no evidence for porous flow of water into boreholes that had been drained of meltwater. However, borehole 4 (BH4; hereafter, all boreholes are similarly abbreviated as designated in Supplementary Table 1) gradually filled during the final two days of observation and samples of the water were collected (Supplementary Fig. 1) on 20 June 2014 (BH4b). From late June to early July 2015, the same location on the glacier was revisited and similar observations were made. Surface melt water subsequently infiltrated two of the boreholes (BH8 and BH9) and only BH10 remained isolated from direct surface input; therefore, it was used as the source for the WCA water samples collected in 2015. BH10 was melted on 25 June 2015, and based on a slow initial rate of refill combined with uncertainly about the contribution of runoff from two days of rainfall, the water was drained after approximately one week and

discarded. Opportunely, subsequent refill of BH10 on three consecutive days (5, 6, and 7 July 2015; samples BH10b, BH10c, and BH10d, respectively; Supplementary Table 1) provided a total of ~110 L of water from the WCA for analyses.

3.2 Physical conditions

A one-dimensional numerical model of heat diffusion, advection, and production was used to create a prediction of temperature (Fig. 1A) and subsurface melt distribution in the ice based on internal heating (Fig. 1B). Modeled temperatures are dominated by the effects of downward propagation of the winter cold wave to depths of ~10 m (Fig. 1A). Somewhat more subtle is the development of an isothermal, temperate summer layer in the top ~2 m of the glacier due to internal heating caused by penetration of solar radiation. Once at the melting point, this layer experiences internal melting resulting in water contents up to 200 L m^{-2} or ~10% by volume (Fig. 1B). The onset of freezing air temperatures in winter quickly eliminates the water-bearing layer in the model.

Comparison of the modeled and observed temperatures (Fig. 1C) shows some similarities and some differences. In July 2015, all three temperature sensors at depths of 15, 25, and 35 m reported the ice to be temperate, ca. 0^{o}C, in spite of the fact that the model predicts temperate conditions only at 35 m depth. During the second half of the record, the observed ice temperatures at 15 m depth drop markedly and reach less than -1^{o}C by early September. At depths of 25 m and 35 m, ice temperatures also drop but much more gradually, and by a smaller magnitude, ca. -0.1^{o}C. Surface observations in this ice marginal study area confirmed the presence of many crevasses and crevasse traces, as well as moulins. Hence, disagreements between modeled and observed temperatures are attributable to the fact that the former does not include such heterogeneities, which may play an important role in transporting water and heat within the ice column. The model also makes no provision for meltwater percolation and storage in intercrystalline veins. Where fast drainage pathways exist (i.e, crevasses and moulins), the meltwater table can drop well below the surface and permit air access and rapid ice cooling, as indicated by the 15 m sensor (Fig. 1C). Heterogeneities enabling advective transport of heat and water significantly alter the simplified picture of physical conditions in near-surface ice, tending to expand the vertical extent of temperate, wet ice beyond the depth of several meters affected by penetration of solar radiation (Fig. 1A). Such heterogeneities would also enable transport of microbial cells and nutrients into deeper ice.

To examine the optical properties of the near-surface ice and its potential to support photosynthetic activity, the diel flux of incident PAR (400-700 nm) and PAR attenuation with ice depth were determined (Fig. 2). Based on mid-afternoon borehole measurements on 16 June 2014, PAR intensity decreases exponentially with ice depth (Fig. 2A) and the PAR attenuation coefficient (K_{PAR}; Hodson et al. 2013) is 1.5 m^{-1}. Comparison

with PAR data for benthic mats (1 μmol m^{-2} s^{-1}; Hawes and Schwarz, 2001) and the water column of highly shaded Antarctic lake ecosystems (0.43 and 0.07 μmol m^{-2} s^{-1}; Priscu et al., 1988) implied that midday PAR fluxes could support photosynthesis to maximum depths of 5 to 7 m (Fig. 2B).

3.3 Chemical composition of the near-surface ice and WCA

A novel ice penetrating cryobot (Stone et al., 2014, 2018) with a water sampling system (Clark et al., 2017) was used to obtain melt water from two boreholes (BH6 and BH7; Supplementary Table 1) located within ~1.5 m of each other, and 24 samples were collected from discrete depths between 1.4 and 8.3 m and filtered for chemical analysis. These data (Supplementary Table 2) indicated that Ca^{2+} was the dominant cation (average of 56 ± 27 ppb; ± standard deviation) and strongly positively correlated (r_s > 0.62, n = 24, p < 0.001) to subordinate K^+, Na^+, Mg^{2+}, Al^{3+}, and $Fe_{(aq)}$ concentrations. Sulfate was the most abundant anion (136 ± 28 ppb) followed by HCO_3^- (75 ± 78 ppb), the latter of which showed large variation with depth (Fig. 3A; Supplementary Table 2). Nitrate and Cl^- exceeded the analytical limit of detection in approximately one-quarter of the samples in the profile, averaging 81 ± 21 and 172 ± 38 ppb, respectively.

Water that percolated into BH10 via porous flow during July 2015 had a pH of 6.2 and 6.8, and conductivity of 12 and 4 μS cm^{-1} (samples BH10b and BH10d, respectively), which is a similar pH but higher conductivity than that observed in supraglacial waters (~1 μS cm^{-1}). Chemical analysis of WCA sample BH10b (Supplementary Table 2) indicated that in contrast to data obtained from ice melt, Na^+ was the dominant cation and Cl^- was the dominant anion. Comparing odds ratios for each analyte indicated that six compounds were substantially enriched (4- to 170-fold; Na^+, K^+, F^-, Al^{3+}, $Fe_{(aq)}$, and Br^-) and five were depleted (3- to 17-fold; SO_4^{2-}, NO_3^-, Cr^{3+}, Pb^{2+}, and Co^{2+}) in the WCA sample relative to average concentrations in ice melt from 1.4 to 8.3 m (Fig. 3B). The largest differences observed between the ice and WCA chemistry were with F^- (170- fold enriched in the WCA), Pb^{2+}, and Co^{2+}, (16- and 17- fold depleted in the WCA, respectively).

3.4 Microbial cells and biomass in the near-surface glacial ice and WCA

The water sampling system of the cryobot was used to collect 45 discrete samples at depths between 1.4 and 11.4 m to estimate the abundance of microbial cells and cellular ATP (Fig. 4A). The Spearman rho value (r_s = 0.38, n = 45) implied a weak positive correlation between the cell and ATP concentration data, but the correlation was not statistically significant (p = 0.066). Nevertheless, the cell and ATP data profile showed similar trends, with the highest concentrations of each at depths of 1.4 to 1.6 m (816 ± 270 cells mL^{-1} and 155 ± 83 amol L^{-1}, n = 5) and lowest values observed at depths > 7.2 m. At depths below 2 m, there were three

horizons (4.0 to 4.1, 6.3 to 6.4, and 8.3 m) where the cell and ATP concentration were higher relative to samples from adjacent depths (Fig. 4A). The cell and ATP data strongly positively correlated with Co^{2+} ($r_s > 0.60$, n = 24, $p < 0.002$) and moderately positively correlated with HCO_3^- ($r_s > 0.47$, n = 24, $p < 0.019$); the ATP concentration also moderately positively correlated with Al^{3+} and K^+ ($r_s > 0.57$, n = 24, $p < 0.004$; Fig. 3A).

The cell concentration in the water generated by melting BH10 (i.e., BH10a) was similar to average values from depths of 1.4 to 11.3 m (Fig. 4C) and 875-fold lower than that observed in supraglacial water (1.92 ± 0.465 × 10^5 cells mL^{-1}). Relative to the 2nd refill event collected on 5 July 2015 (BH10b; 2,760 ± 488 cells mL^{-1}), subsequent sampling on consecutive days (6 and 7 July 2015; samples BH10c and BH10d, respectively) revealed that cell concentrations in the 3rd and 4th refills were 78% and 93% lower, respectively (Fig. 4C). The ATP concentration in water sampled from the 3rd refill (BH10c) was 32 ± 3.4 amol L^{-1} and slightly lower than the average for depths of 1.4 to 11.3 m (54 ± 50 amol L^{-1}; Fig. 4A).

3.5 Microbial respiration and oxygen consumption

The respiration potential of microorganisms in the WCA was evaluated in June 2014 by measuring the reduction of XTT [2,3-Bis(2-methoxy-4-nitro-5- sulfophenyl)-2H-tetrazolium-5- carbox-anilide] during time-course experiments that were incubated at a depth of 1.5 m in a packered borehole. Sample for the rate measurement was obtained from water in BH5, which was melted one day prior to the experiment. To investigate if the respiration rate was affected by PAR availability at 1.5 m (Fig. 2), identical preparations of the samples were incubated in situ in the light and dark. Under both conditions, the production of formazan at the in situ temperature was linear over 5.5 h (Fig. 5A), and the slope of the data from the light ($b_{light} = 0.0691$) was slightly higher than that in the dark ($b_{dark} = 0.0610$), but formazan production was not statistically different between the treatments (Student's t-distribution, $p = 0.46$, n = 29).

During July 2015, water collected from the 3rd refill event in BH10 (sample BH10c) was found to be under-saturated with respect to oxygen (11.6 ± 0.3 mg L^{-1}, 88% of air-saturated water). To estimate the oxygen uptake rate in the WCA, the BH10c samples were sealed in serum bottles with no headspace and incubated ex situ at 5°C in the dark and light (~270 μmol photons m^2 s^{-1}) for 117 and 97 days, respectively. The rate of oxygen consumption during these experiments (Fig. 5B) was modeled as a first order decay process and revealed that samples incubated in the light had a larger reaction rate coefficient (k = 0.0167 d^{-1}, R^2= 0.644) than those in the dark (k = 0.00553 d^{-1}, R^2= 0.676). Data from the first 32 days of incubation were used to calculate the initial rate of consumption in the light and dark (152 and 70 μg O_2 L^{-1} d^{-1}, respectively), and the linear regression models for these conditions had significantly different slopes ($p = 0.010$, n = 24). Correction of the

rate data to the in situ temperature of 0°C (Fig. 1A) provided oxygen consumption estimates of 42 and 92 μg O^2 L^{-1} d^{-1} in the dark and light, respectively.

The WCA sample used for the ex situ incubations (BH10c) had an initial cell density of 620 ± 130 cells mL^{-1} (Fig. 4C). To confirm that oxygen consumption was associated with microbial growth, the cell concentration was determined approximately midway (60 and 46 d for dark and light incubations, respectively) and at the termination of the experiment. Over the time course shown in Fig. 5B, cell density increased by three orders of magnitude and was 6.3 ± 0.58 × 10^5 and 5.9 ± 0.45 × 10^5 cells mL^{-1} for samples incubated in the dark and light, respectively. Assuming exponential growth during the first half of the experiment, the mean doubling time of the populations at 0°C was estimated at 14 and 11 days in the dark and light, respectively.

3.6 Composition of microbial assemblages in the near-surface ice and WCA ecosystem

A total yield of ≤ 200 pg (i.e., limit of detection for the DNA quantification method) to 200 ng of genomic DNA was obtained from the filter samples extracted, a portion of which was used to amplify the V4 region of the 16S rRNA gene. Amplicons obtained from 31 samples (Supplementary Table 3) and four procedural controls (three DNA extraction blanks and a PCR control, all amplified using 45 cycles) were sequenced, producing 14,349,197 paired-end contigs with an average read length of 253 bp. After quality filtering and removing chimeras and singletons, 10,024,390 sequences remained that classified as 12,970 OTUs. OTUs that co-occurred in the procedural control data at abundances > 0.05% of total sequences (279 OTUs) were designated as experimental contaminants and removed from the dataset, leaving 7,754,705 unique reads for evaluation. Each sample was normalized to 9,151 sequences, reducing the dataset to 283,681 sequences that classified as 3,381 OTUs. Abundant OTUs were defined as having relative abundances ≥0.1% of total sequences and represented between 65% and 99% of the OTUs in each sample. Based on Good's coverage estimates for the normalized sequences (> 0.96; Supplementary Table 3), the data are sufficient to describe the most abundant taxa in the samples.

The abundant OTUs in the samples classify within 9 bacterial phyla: Proteobacteria were the dominant phylum, followed by Cyanobacteria, Bacteroidetes, Actinobacteria, Armatimonadetes, Firmicutes, Acidobacteria, Deinococcus, and candidate phylum WPS-2 (8 bacterial OTUs could not be classified at the phylum level). Based on the NMDS analysis (Fig. 6A), the samples cluster into three highly significantly different groups (AMOVA; $p \leq 0.001$, $n = 31$) that can be generally characterized as: i) 2014 samples from boreholes of 10 to 30 m depth (top right of plot), ii) 2015 samples collected at discrete depths between 2 to 15 m (top left), and iii) samples heavily influenced by surface and in-ice melting (i.e., stream and WCA water; bulk ice melt from boreholes ≤ 4 m; bottom of Fig. 6A). The vast majority of sequences in the englacial 2014

samples from borehole depths of 10 to 30 m were proteobacterial (94% of the sequences), with taxa in the Actinobacteria (3%), Bacteroidetes (1%), Cyanobacteria (1%), and 6 other phyla comprising the remainder (Supplementary Fig. 2). Samples from the deepest 2015 boreholes had similar phyla distributions; however, the 2014 samples were dominated by Gammaproteobacteria whereas betaproteobacterial OTUs were more abundant in the 2015 data. This contrasted to the assemblages in the near-surface samples, which were comprised of OTUs affiliated with the phyla Proteobacteria (39%), Cyanobacteria (22%), Bacteroidetes (18%), Actinobacteria (9%), Armatimonadetes (2%), Acidobacteria (1%), Deinococcus/Thermus (1%), and candidate phylum WPS-2 (<0.5%; Supplementary Fig. 2).

To explore the provenance of species in the glacier's near-surface and ascertain if the observed distributions were consistent with the release of microbes from englacial ice during melting, an odds ratio for each OTU was calculated by comparing abundance with data from the deepest boreholes (Fig. 6B). For the 2014 samples, OTU abundances in samples BH3, BH4a, and BH5 were compared to data from BH2 (n=8; Supplementary Table 3). Similarly, samples from shallow 2015 boreholes (BH9 and BH10a) were compared with data from BH6, BH7, and BH8 (n=7). Based on this approach, 23 OTUs in seven bacterial phlya were identified that had > 5-fold higher abundances in the glacier's near-surface (Fig. 6B) and represented approximately one-third of the sequences in these samples. Most of these OTUs classify as Alphaproteobacteria, Bacteroidetes, and Cyanobacteria, with the nearest neighbors for three of the five cyanobacterial OTUs being the 16S rRNA sequences of plastids most closely related to those possessed by chrysophyte and streptophyte algal species (Supplementary Fig. 3). Several of the plastid 16S rRNA sequences were the most abundant OTUs in the near-surface samples (OTU8 and OTU9 together make up 16% of the 2014 and 11% of the 2015 data). DNA from BH10d was used to amplify and clone a portion of the 18S rRNA gene for phylogenetic analysis. Sequencing of 25 clones identified 3 OTUs related to green and golden algae (Fig. 6C) as well as 4 OTUs related to fungal, ciliate, and rotifer species (Supplementary Table 4). The phylogenetic relationships of the 18S rRNA gene sequences related to members of the classes Zygnematophyceae and Chrysophyceae (Fig. 6C) was consistent with the composition of algal taxa inferred based on the plastid 16S rRNA gene data (Supplementary Fig. 3).

4 Discussion

Near-surface internal melting of glacial ice provides liquid water for microbial metabolism and promotes meltwater percolation that can transport solutes, gases, organic matter, and cells both vertically and horizontally

through a highly permeable ice layer (Irvine-Fynn et al., 2012; Cook et al., 2016). To investigate the parameters influencing the transformation of polycrystalline ice into a perched aquifer and biogeochemically-active habitat during the ablation season, a one-dimensional heat conduction-production model was used to examine the effect of temperature and solar radiation on water availability in the ice. Elevated air temperatures during summer combined with heat from the dissipation of shortwave radiation produce a ~2 m solar weathering crust that contained a meltwater fraction as high as 10% of the ice by volume (Fig. 1). The depth of meltwater production inferred by the model is consistent with observations from High Arctic glaciers (Irvine-Fynn and Edwards, 2014) but exceeds that for Antarctic dry valley glaciers by more than 10-fold (5-15 cm; Hoffman et al., 2014) because the ice is much colder and penetrating radiation is used to warm ice rather than melt it. Although the low-density surface ice can serve as a reservoir for 14-18 cm of meltwater (Cooper et al. 2018), the low hydraulic conductivities observed for northern hemisphere glaciers indicate that meltwater flow through the WCA is slow and inefficient (Stevens et al. 2018).

Irvine-Fynn and Edwards (2014) speculated that environmental conditions in the WCA facilitate biogeochemical processing by providing microbes with access to light, effectively extending a glacier's "photic zone" to depths beneath the surface. The PAR attenuation coefficient derived for surface ice of the Matanuska Glacier during summer 2014 (K_{PAR} = 1.5 m^{-1}) indicates higher light propagation with depth compared to wet or dry snow (K_{PAR} = 7.5 to 20 m^{-1}) and is similar to values reported for lake, sea, and blue ice (Hodson et al., 2013 and references within). Based on the photosynthetic properties of highly shaded polar aquatic ecosystems (Priscu et al., 1988; Hawes and Schwarz, 2001), sufficient PAR may penetrate to ice depths of 5 to 7 m during daily maximums to support cyanobacterial and algal photosynthesis (Fig. 2B). However, since the solar radiation flux is incapable of producing appreciable meltwater at depths > 2 m (Fig. 1A), photosynthetic and microbial activity are likely localized to the near-surface region. The upper 2 m of ice experiences at least 3% of the surface PAR flux (Fig. 2A) and may hold up to 200 L of liquid water per square meter of glacier surface during the peak of the melt season (Fig. 1B). Remarkably, if the WCA community possesses species capable of acclimating to highly shaded conditions, such as those found in ice-covered Antarctic lakes (0.07 μmol m^{-2} s^{-1}; Priscu et al., 1988), then the diel pattern observed during civil twilight implies the PAR flux continually exceeded the threshold necessary to support photosynthetic activity (Fig. 2B).

The oxygen uptake rate for WCA samples incubated in the light (92 μg O_2 L^{-1} d^{-1}; Fig. 5B) was more than twice values obtained in the dark (42 μg O_2 L^{-1} d^{-1}) and ~5-fold lower than estimates in supraglacial melt ponds in proximity to the study site (440 to 600 μg O_2 L^{-1} d^{-1} under ambient light; data not shown). Similar measurements in most aquatic ecosystems typically observe higher dissolved oxygen concentrations when

samples are incubated in the light due to stimulation of oxygenic photosynthetic activity. Pace and Prairie (2005) and Abbasi and Chari (2008) offer four possible explanations germane to interpreting these results. First, the photochemical oxidation of inorganic or organic compounds consumes oxygen and cannot be discounted as a sink in these experiments. Nevertheless, cell growth was observed in the microcosm studies and the populations had shorter generation times in light versus dark incubations (11 and 14 days, respectively). Second, samples incubated in the light may experience higher incubation temperatures, but this possibility can be excluded because the dark samples were wrapped in aluminum foil and incubated under illumination, making uniform temperature differences between treatments unlikely. Finally, oxygen may be consumed by phototrophic algae and cyanobacteria through pseudocyclic electron transport (i.e., the Mehler reaction) or by the CO_2-fixing enzyme RuBisCO (ribulose-1,5-bisphosphate carboxylase/oxygenase) during photorespiration. Given the high proportion of phototrophic taxa detected in the near surface samples (Supplementary Fig. 2), these latter mechanisms provide the most plausible explanation for the elevated oxygen consumption rates during light incubation (Fig. 5B).

Meltwater production and duration in the ice are highly relevant to microbial processes in the WCA. Modeling of the ice properties under the local meteorological conditions from 2014 to 2016 suggests water content in the weathering crust increased gradually with the onset of the ablation season and that a substantial fraction of this water persisted in the ice for ~7.5 months each year (Fig. 1). Snow cover is not included in our simulations but its two main effects may cancel each other out. Snow on ice acts as a thermal insulator, decreasing the cooling effect of the winter cold wave propagating into the near-surace zone. In late spring and early summer, snow will hinder penetration of sunlight, ice warming, and generation of internal melt. Therefore, we conjecture that the two effects may impact more the timing of the beginning and the end of the seasonal WCA rather than its overall duration. Acknowledging that ex situ assays may allow microbial populations to enumerate at rates higher than those in situ (i.e., the bottle effect), the maximum generation times observed (2 weeks) coupled with the duration of the meltwater interval implies that 16 generations per year were possible. Assuming retention of the cells in the surface during summer (Irvine-Fynn et al., 2012), the potential for WCA communities to increase total biomass by four orders of magnitude (i.e., 2^{16}) each melt season is a level of production that could significantly influence the carbon cycling budgets of ecosystems directly associated with the glacier and its drainage system (Anesio et al., 2010).

The availability of biologically labile organic carbon in WCA samples was supported by no observable lag in the time-dependent reduction of XTT to its formazan product (Fig. 5A) and also demonstrated the presence of cells with active respiratory chains and electron donors to drive oxidative phosphorylation. Elevated

cell and ATP concentrations (Fig. 4A) were observed at depths with the highest predicted water contents (Fig. 1) and positively correlated with the concentration of bicarbonate (Fig. 3A), consistent with in situ microbial respiration and growth in the WCA. Several horizons below predicted depths of meltwater production showed relative increases in the concentration of cells and ATP (i.e., 4.0 to 4.1, 6.3 to 6.4, and 8.3 m; Fig. 4A), but the microbial assemblages detected at these depths were distinctly different from those in the near-surface ice (Fig. 6A). Hence, we conclude that these represent cell populations that were deposited on the glacier's surface at a time in the past, became archived within the ice chronology, and glacier movement conveyed to the ablation zone. The positive correlation of the cell and ATP data with Al^{3+} and K^{+} likely reflect contributions from aeolian transport to the ice surface and subsequent weathering, but the data for Co^{2+} (Fig. 3A) are interesting when juxtaposed with the results of Taylor and Sullivan (2008). This study showed that uptake of Co^{2+} and vitamin B_{12} synthesis by bacteria in Antarctic sea ice supplied this vital micronutrient to algae auxotrophic for B_{12}. Consequently, the higher concentrations of Co^{2+} observed in the weathering crust (Fig. 3A; Supplementary Table 2) could be associated with community micronutrient recycling. Interactions between phototrophic and heterotrophic guilds in this sympagic environment should be enhanced by the close proximity offered on cell-particle aggregates (Fig. 4B), and those observed shared characteristics similar to those reported in the ice covers of Antarctic dry valley lakes (Priscu et al., 1998), cryoconite holes (Hodson et al., 2010; Langford et al., 2010), and sea ice (Riebesell et al., 1991).

Surface water transport and emergence of ice in the actively melting ablation area are the processes most likely providing microbial inoculum to the WCA. According to NMDS ordination, microbial assemblages in the deepest boreholes (i.e., originating from englacial ice) clustered by year and were highly significantly different from samples in the glacier's near-surface (Fig. 6A). Considering ablation rates of 4 to 15 cm day^{-1} at the Matanuska Glacier during May to August (Ensminger et al., 1999; Reynolds, 2005; Mankoff and Russo, 2013), most of the ice column sampled in 2014 would have ablated by the following season (i.e., relative to the ice surface in 2014, the samples collected in 2015 originated from a deeper horizon in the glacier). Curiously, data from a 10 m borehole (BH1) on two consecutive days in 2014 (BH1a and BH1b) clustered with near-surface ice samples, but the assemblages observed on the third day (BH1c) were more similar to those in the deeper 2014 boreholes (Fig. 6A). Movement of the glacier over irregular terrain has highly fractured the ice in the marginal area studied, and the hydrologically-connected fracture networks of temperate glaciers link the near-surface to the englacial zone (Fountain et al., 2005). The temporal changes observed in BH1 support the possibility that microbes originating from deeper portions of the ice column can be mobilized and englacially transported with water on relatively short time frames.

Microbial communities in the 2014 and 2015 samples from shallow boreholes (4 m), a supraglacial stream, and the WCA formed a loose cluster in NMDS ordination space (Fig. 6A). Comparison of bulk meltwater (BH4a and BH10a) with water that subsequently percolated into the boreholes (BH4b, BH10b, BH10c, and BH10d) indicated no significant difference in community structures (p = 0.138, n = 6). The community in the first WCA sample collected in 2015 (BH10b) was considerably less diverse than that in the borehole meltwater (BH10a; Fig. 4C), plotted on the periphery of the near-surface cluster in NMDS analysis (Fig. 6A), and had a structure significantly different from the other WCA samples (p = 0.015, n = 6). However, samples collected from BH10 over the following two days (BH10c and BH10d) contained more diverse communities (Fig. 4C) that were more similar to each other and the 2014 WCA sample BH4b (Fig. 6A). Sample BH10b was collected after a period of rainfall, contained a cell concentration 5- to 14-fold higher than the other WCA samples (Fig. 4C), and was highly enriched with two gammaproteobacterial OTUs in the genera *Pseudomonas* and *Stenotrophomonas* that comprised 54% of the sequences. Together, the data from BH10 provide anecdotal evidence for a hydrologic response to precipitation that enhanced the mobilization of microbes from other hydrogeological regions and/or facilitated the transfer of species deposited in rain to the WCA.

If the WCA represents an ecotone between the supraglacial and englacial environment, then the presence of distinct species and community structures would be expected. However, a strict interpretation of the WCA community composition based on data from the percolating water may be complicated by the co-occurrence of microbes in the samples that originated from aquatic ecosystems on the surface, glacial ice melt, and wet or dry deposition. Odds ratios derived from sequence abundances (Fig. 6B) indicate that 23 OTUs affiliated with eight bacterial phyla and the plastids of golden and green algae (Supplementary Fig. 3) were enriched more than five-fold in the WCA relative to englacial ice samples. Four of these OTUs (OTU21, 31, 48, and 53) were at abundances >1% of the sequences in the WCA and near-surface ice samples but represented <0.1% of the sequences in supraglacial water, suggestive for the presence of distinct OTUs in the weathering crust. The largest odds ratios were observed for deltaproteobacterial OTUs in the 2014 samples, but three OTUs with high identity to plastid 16S rRNA gene sequences of Zygnematophyceae and Chrysophyceae taxa (OTU8, 9, and 48) had odds ratios that ranged from 5 to 35 during both years (Fig. 6B) and represented 11 to 16% of sequences detected in the near-surface ice samples (BH3, BH4a, BH5, BH9, and BH10a). Phylogenetic analysis of 18S rRNA gene sequences amplified from a WCA sample revealed OTUs closely related to snow and ice algae in the genera *Ancylonema, Mesotaenium,* and *Ochromonas* (Fig. 6C; Supplementary Table 4). Previous studies have identified *Ancylonema nordenskioldii* and *Mesotaenium breggrenii* in Matanuska Glacier

cryoconites near the terminus (Takeuchi et al., 2003) as well as on the surface of the Greenland and Antarctic ice sheets (Anesio et al., 2017; Lutz et al., 2018).

5 Conclusions

During the ablation season, microbes in the glacial weathering crust are provided with liquid water, solar radiation, oxygen, and conditions suitable for biogeochemical processing. Though phototrophic activity contributes new organic carbon and generates oxygen to drive heterotrophic metabolisms, primary producers and consumers in the WCA must acquire other vital nutrients to support growth, which are primarily sourced from melting glacial ice and co-transported with percolating surface water. Biomass turnover in the WCA would also mineralize and mobilize nutrients, and thus, could have important roles in fertilizing supraglacial biological activity. Although the WCA of temperate glaciers can provide a liquid water oasis in the ice for over half the annual cycle, decreased solar irradiance and temperature at the onset of winter leads to freezing, entrapping the microbial community in a near-surface refuge. Hence, surviving fractions of these populations could then serve as inocula for microbial community development during the subsequent season. Since the hydrological transport of nutrient-laden meltwater may fertilize ecosystems associated with the ice surface, subglacial environments, and proglacial streams, elucidating the factors affecting biogeochemical flux and cycling in WCA ecosystems warrants more detailed investigation.

Data availability: The 16S rRNA gene sequence data are deposited in the National Center for Biotechnology Information's Sequence Read Archive (project number SRP130982). The cloned 18S rRNA gene sequence data are assigned the GenBank accession numbers MH037315 to MH037321.

Supplement link: The Supplement related to this article is available online at: TBD

Author contributions: B.C.C., S.M.T., P.T.D., and W.C.S. designed the research; B.C.C., H.F.L., C.L.D., E.E.O., S.U.N., K.F.M., S.M.T., and P.T.D. performed the research; B.H. conducted analytical analysis; W.C.S. developed and provided technological resources; B.C.C., C.L.D., S.M.T., and P.T.D. analyzed the data; and B.C.C. wrote the manuscript with contributions from all authors.

Competing interests: The authors declare no conflict of interest.

Acknowledgements: This research was supported by a grant from the NASA ASTEP Program (NNX11AJ89G). Partial support was also provided by the Institute of Food and Agricultural Sciences at the University of Florida. We thank J. Farrar for assistance with extracting samples for nucleic acid analysis and J. Cook, A. Hodson, and J. Priscu for discussion. Support and assistance provided by the following 2014 and 2015 VALKYRIE field team members was crucial to the success of this research: N. Bramall, E. Clark, C. Flesher, J. Harman, B. Hogan, J. Moor, D. Rickel, D. Sampson, V. Siegel, and V. Yuan.

References

Abbasi, S.A. and Chari, K.B: Environmental management of urban lakes: with special reference to Oussudu. Discovery Publishing House, 2008.

Anesio, A.M., Hodson, A.J., Fritz, A., Psenner, R. and Sattler, B.: High microbial activity on glaciers: importance to the global carbon cycle. Glob. Chang. Biol., 15, 955-960, https://doi.org/10.1111/j.1365-2486.2008.01758.x, 2009.

Anesio, A.M., Lutz, S., Christmas, N.A.M., and Benning, L.G: The microbiome of glaciers and ice sheets. NPJ Biofilms Microbiomes, 3, 10, https://doi.org/10.1038/s41522-017-0019-0, 2017.

Anesio, A.M., Sattler, B., Foreman, C., Telling, J., Hodson, A., Tranter, M. and Psenner, R.: Carbon fluxes through bacterial communities on glacier surfaces. Annals of Glaciology, 51, 32-40, https://doi.org/10.3189/172756411795932092, 2010.

Arcone, S.A., Lawson, D.E., and Delaney, A.J.: Short-pulse radar wavelet recovery and resolution of dielectric contrasts within englacial and basal ice of Matanuska Glacier, Alaska, USA. J. Glaciol., 41, 68-86, https://doi.org/10.3189/S0022143000017779, 1995.

Bamber, J.L. and Aspinall, W.P: An expert judgement assessment of future sea level rise from the ice sheets. Nat. Clim. Chang., 3, 424-427, http://dx.doi.org/10.1038/nclimate1778, 2013.

Bolger, A.M., Lohse, M., and Usadel, B.: Trimmomatic: A flexible trimmer for Illumina sequence data. Bioinformatics 30, 2114-2120, https://doi.org/10.1007/s12686-017-0754-9, 2014.

Caporaso, J.G., Lauber, C.L., Walters, W.A., Berg-Lyons, D., Huntley, J., Fierer, N., Owens, S.M., Betley, J., Fraser, L., Bauer, M., and Gormley, N.: Ultra-high-throughput microbial community analysis on the Illumina HiSeq and MiSeq platforms. ISME J., 6, 1621-1624, http://dx.doi.org/10.1038/ismej.2012.8, 2012.

Christner, B.C., Priscu, J.C., Achberger, A.M., Barbante, C., Carter, S.P., Christianson, K., Michaud, A.B., Mikucki, J.A., Mitchell, A.C., Skidmore, M.L. Vick-Majors, T.J., and the WISSARD Science Team: A microbial ecosystem beneath the West Antarctic Ice Sheet. Nature, 512, 310-313, http://dx.doi.org/10.1038/nature13667, 2014.

Chu, V. W.: Greenland ice sheet hydrology: a review. Prog. Phys. Geogr., 38, 19-54, https://doi.org/10.1177/0309133313507075, 2014.

Clark, E.B., Bramall, N.E., Christner, B., Flesher, C., Harman, J., Hogan, B., Lavender, H., Lelievre, S., Moor, J., Siegel, V., and Stone, W.C.: An intelligent algorithm for autonomous scientific sampling with the VALKYRIE cryobot. Int. J. Astrobiol., doi:10.1017/S1473550417000313, 2017.

Cook, J.M., Hodson, A.J., and Irvine-Fynn, T.D.: Supraglacial weathering crust dynamics inferred from cryoconite hole hydrology. Hydrol. Process., 30, 433-446, https://doi.org/10.1002/hyp.10602, 2016.

Cooper, M.G., Smith, L.C., Rennermalm, A.K., Miège, C., Pitcher, L.H., Ryan, J.C., Kang, Y. and Cooley, S.W.: Meltwater storage in low-density near-surface bare ice in the Greenland ice sheet ablation zone. The Cryosphere, 12, 955-970, https://doi.org/10.5194/tc-12-955-2018, 2018.

Dee, D.P., Uppala, S.M., Simmons, A.J., Berrisford, P., Poli, P., Kobayashi, S., Andrae, U., Balmaseda, M.A., Balsamo, G., Bauer, P., Bechtold, P., Beljaars, A.C.M., van de Berg, L., Bidlot, J., Bormann, N., Delsol, C., Dragani, R., Fuentes, M., Geer, A.J., Haimberger, L., Healy, S.B., Hersbach, H., Hólm, E.V., Isaksen, L., Kållberg, P., Köhler, M., Matricardi, M., McNally, A.P., Monge-Sanz, B.M., Morcrette, J.-J., Park, B.-K., Peubey, C., de Rosnay, P., Tavolato, C., Thépaut, J.-N., Vitart, F.: The ERA-Interim reanalysis: configuration and performance of the data assimilation system. Q. J. R. Meteorol. Soc., 137, 553–597, https://doi.org/10.1002/qj.828, 2011.

Edwards, A. and Cameron, K. A. Microbial life in supraglacial environments. In: Psychrophiles: From Biodiversity to Biotechnology, Ch. 4. Springer, Cham, 2017.

Ensminger, S.L., Evenson, E.B., Larson, G.J., Lawson, D.E., Alley, R.B., and Strasser, J.C.: Preliminary study of laminated, silt-rich debris bands: Matanuska Glacier, Alaska, USA. Annals of Glaciology, 28, 261-266, https://doi.org/10.3189/172756499781821850, 1999.

Fitzpatrick, A.A.W., Hubbard, A.L., Box, J.E., Quincey, D.J., Van As, D., Mikkelsen, A.P.B., Doyle, S.H., Dow, C.F., Hasholt, B., and Jones, G.A.: A decade (2002-2012) of supraglacial lake volume estimates across Russell Glacier, West Greenland. The Cryosphere, 8, 107-121, https://doi.org/10.5194/tc-8-107-2014, 2014.

Fountain, A.G., Jacobel, R.W., Schlichting, R., and Jansson, P.: Fractures as the main pathways of water flow in temperate glaciers. Nature, 433, 618-621, http://dx.doi.org/10.1038/nature03296, 2005.

Gardner, A.S. and Sharp, M.J.: A review of snow and ice albedo and the development of a new physically based broadband albedo parameterization. J. Geophys. Res. Earth Surf., 115, F01009, https://doi.org/10.1029/2009JF001444, 2010.

Hadziavdic, K., Lekang, K., Lanzen, A., Jonassen, I., Thompson, E.M. and Troedsson, C.: Characterization of the 18S rRNA gene for designing universal eukaryote specific primers. PLoS ONE, 9, e87624, https://doi.org/10.1371/journal.pone.0087624, 2014.

Hawes, I. and Schwarz, A.M.: Absorption and utilization of irradiance by cyanobacterial mats in two ice-covered Antarctic lakes with contrasting light climates. J. Phycol., 37, 5-15, https://doi.org/10.1046/j.1529-8817.1999.014012005.x, 2001.

Hodson, A., Cameron, K., Bøggild, C., Irvine-Fynn, T., Langford, H., Pearce, D., and Banwart, S.: Glacial ecosystems. Ecol. Monogr., 78, 41-67, https://doi.org/10.1890/07-0187.1, 2008.

Hodson, A., Cameron, K., Bøggild, C., Irvine-Fynn, T., Langford, H., Pearce, D. and Banwart, S.: The structure, biological activity and biogeochemistry of cryoconite aggregates upon an Arctic valley glacier: Longyearbreen, Svalbard. J. Glaciol. 56, 349-362, https://doi.org/10.3189/002214310791968403, 2010.

Hodson, A., Paterson, H., Westwood, K., Cameron, K., and Laybourn-Parry, J.: A blue-ice ecosystem on the margins of the East Antarctic Ice Sheet. J. Glaciol., 59, 255-268, https://doi.org/10.3189/2013JoG12J052, 2013.

Hoffman, M.J., Fountain. A.G., and Liston, G.E.: Near-surface internal melting: a substantial mass loss on Antarctic Dry Valley glaciers. J. Glaciol., 60, 361-374, https://doi.org/10.3189/2014JoG13J095, 2014.

Hopes, A., Thomas, D.N., and Mock, T.: Polar microalgae: functional genomics, physiology, and the environment. In: Psychrophiles: From Biodiversity to Biotechnology, Ch. 14. Springer, Cham, 2017.

Irvine-Fynn, T.D.L., Edwards, A., Newton, S., Langford, H., Rassner, S.M., Telling, J., Anesio, A.M. and Hodson, A.J.: Microbial cell budgets of an Arctic glacier surface quantified using flow cytometry. Environ. Microbiol., 14, 2998-3012, https://doi.org/10.1111/j.1462-2920.2012.02876.x, 2012.

Irvine-Fynn, T.D. and Edwards, A.: A frozen asset: the potential of flow cytometry in constraining the glacial biome. Cytometry A, 85, 3-7, https://doi.org/10.1002/cyto.a.22411, 2014.

Karlstrom, L., Zok, A., and Manga, M.: Near-surface permeability in a supraglacial drainage basin on the Llewellyn Glacier, Juneau Icefield, British Columbia. The Cryosphere, 8, 537-546, https://doi.org/10.5194/tc-8-537-2014, 2014.

Kumar, S., Stecher, G., and Tamura, K.: MEGA7: Molecular Evolutionary Genetics Analysis version 7.0. Mol. Biol. Evol., 33, 1870-1874, https://doi.org/10.1093/molbev/msw054, 2016.

LaChapelle, E.: Errors in ablation measurements from settlement and sub-surface melting. J. Glaciol., 3, 458–467, https://doi.org/10.3198/1959JoG3-26-458-467, 1959.

Langford, H., Hodson, A., Banwart, S., and Bøggild, C.: The microstructure and biogeochemistry of Arctic cryoconite granules. Annals of Glaciology, 51, 87-94, https://doi.org/10.3189/172756411795932083, 2010.

Langley, E. S., Leeson, A. A., Stokes, C. R., and Jamieson, S. S.: Seasonal evolution of supraglacial lakes on an East Antarctic outlet glacier. Geophys. Res. Lett., 43, 8563-8571, https://doi.org/10.1002/2016GL069511, 2016.

Lutz, S., McCutcheon, J., McQuaid, J.B., and Benning, L.G.: The diversity of ice algal communities on the Greenland Ice Sheet as revealed by oligotyping. Microb. Genom., 4, https://dx.doi.org/10.1099/mgen.0.000159, 2018.

Mankoff, K.D. and Russo, T.A.: The Kinect: A low-cost, high-resolution, short-range 3D camera. Earth Surface Processes and Landforms, 38, 926-936, https://doi.org/10.1002/esp.3332, 2013.

Müller, F. and Keeler, C.M.: Errors in short-term ablation measurements on melting ice surfaces. J. Glaciol., 8, 91-105, https://doi.org/10.3189/S0022143000020785, 1969.

Munro, D. S.: Comparison of melt energy computations and ablatometer measurements on melting ice and snow. Arct. Alp. Res., 22, 153–162, https://doi.org/10.2307/1551300, 1990.

Munro, D.S.: Delays of supraglacial runoff from differently defined microbasin areas on the Peyto Glacier. Hydrological Processes, 25, 2983-2994, https://doi.org/10.1002/hyp.8124, 2011.

Pace, M.L. and Prairie, Y.T. Respiration in lakes. In: Respiration in aquatic ecosystems, 103-122. Oxford Univ. Press, Oxford, 2005.

Priscu, J.C., Fritsen, C.H., Adams, E.E., Giovannoni, S.J., Paerl, H.W., McKay, C.P., Doran, P.T., Gordon, D.A., Lanoil, B.D. and Pinckney, J.L.: Perennial Antarctic lake ice: an oasis for life in a polar desert. Science, 280, 2095-2098, https://doi.org/10.1126/science.280.5372.2095, 1998.

Priscu, J.C., Priscu, L.R., Howard-Williams, C., and Vincent, W.F.: Diel patterns of photosynthate biosynthesis by phytoplankton in permanently ice-covered Antarctic lakes under continuous sunlight. J. Plankton. Res., 10, 333-340, https://doi.org/10.1093/plankt/10.3.333, 1988.

Priscu, J.C. Limnological methods for the McMurdo Long Term Ecological Research Program. http://mcm.lternet.edu/sites/default/files/MCM_Limno_Methods_AC_23_Oct_2013.pdf, 2013.

Pruesse, E., Peplies, J., and Glöckner, F.O.: SINA: accurate high-throughput multiple sequence alignment of ribosomal RNA genes. Bioinformatics, 28, 1823-1829, https://doi.org/10.1093/bioinformatics/bts252, 2012.

R Core Team: R: A language and environment for statistical computing. R Foundation for Statistical Computing, Vienna, Austria, https://www.R-project.org/, 2017.

Rassner, S.M., Anesio, A.M., Girdwood, S.E., Hell, K., Gokul, J.K., Whitworth, D.E., and Edwards, A.: Can the bacterial community of a High Arctic glacier surface escape viral control? Front. Microbiol., 7, 956, https://dx.doi.org/10.3389%2Ffmicb.2016.00956, 2016.

Reynolds, H.: Evaluation of relationships between supraglacial stream discharge, ablation rates, and climate conditions at the Matanuska Glacier, Alaska. Geological Society of America Abstracts with Programs, 37, 84, 2005.

Riebesell, U., Schloss, I., and Smetacek, V.: Aggregation of algae released from melting sea ice: implications for seeding and sedimentation. Polar Biol., 11, 239-248, https://doi.org/10.1007/BF00238457, 1991.

Roslev, P. and King, G.M.: Application of a tetrazolium salt with a water-soluble formazan as an indicator of viability in respiring bacteria. Appl. Environ. Microbiol., 59, 2891-2896, 1993.

Schloss, P.D., Westcott, S.L., Ryabin, T., Hall, J.R., Hartmann, M., Hollister, E.B., Lesniewski, R.A., Oakley, B.B., Parks, D.H., Robinson, C.J., and Sahl, J.W.: Introducing mothur: open-source, platform-independent, community-supported software for describing and comparing microbial communities. Appl. Environ. Microbiol., 75, 7537-7541, https://doi.org/10.1128/AEM.01541-09, 2009.

Scott, D., Hood, E. and Nassry, M.: In-stream uptake and retention of C, N and P in a supraglacial stream. Annals of Glaciology, 51, 80-86, https://doi.org/10.3189/172756411795932065, 2010.

Smith, L.C., Chu, V.W., Yang, K., Gleason, C.J., Pitcher, L.H., Rennermalm, A.K., Legleiter, C.J., Behar, A.E., Overstreet, B.T., Moustafa, S.E. and Tedesco, M.: Efficient meltwater drainage through supraglacial streams and rivers on the southwest Greenland ice sheet. Proc. Natl. Acad. Sci. USA, 112, 1001-1006, https://doi.org/10.1073/pnas.1413024112, 2015.

Smith, L.C., Yang, K., Pitcher, L.H., Overstreet, B.T., Chu, V.W., Rennermalm, Å.K., Ryan, J.C., Cooper, M.G., Gleason, C.J., Tedesco, M. and Jeyaratnam, J.: Direct measurements of meltwater runoff on the Greenland ice sheet surface. Proc. Natl. Acad. Sci. USA, 114, E10622-E10631, https://doi.org/10.1073/pnas.1707743114, 2017.

Sole, A.J., Mair, D.W.F., Nienow, P.W., Bartholomew, I.D., King, M.A., Burke, M.J. and Joughin, I.: Seasonal speedup of a Greenland marine‐terminating outlet glacier forced by surface melt–induced changes in subglacial hydrology. J. Geophys. Res. Earth Surf., 116, F03014, https://doi.org/10.1029/2010JF001948, 2011.

Stevens, I.T., Irvine-Fynn, T.D., Porter, P.R., Cook, J.M., Edwards, A., Smart, M., Moorman, B.J., Hodson, A.J. and Mitchell, A.C.: Near-surface hydraulic conductivity of northern hemisphere glaciers. Hydrol. Process., 32, 850-865, https://doi.org/10.1002/hyp.11439, 2018.

Stibal, M., Box, J.E., Cameron, K.A., Langen, P.L., Yallop, M.L., Mottram, R.H., Khan, A.L., Molotch, N.P., Chrismas, N.A., Calì Quaglia, F. and Remias, D.: Algae drive enhanced darkening of bare ice on the Greenland ice sheet. Geophys. Res. Lett., 44, 11463–11471, https://doi.org/10.1002/2017GL075958, 2017.

Stone, W.C., Hogan, B., Siegel, V., Lelievre, S., and Flesher, C.: Progress towards an optically powered cryobot. Annals of Glaciology, 55, 1-13, https://doi.org/10.3189/2014AoG65A200, 2014.

Stone, W., Hogan, B., Siegel, V., Harman, J., Flesher, C., Clark, E., Pradhan, O., Gasiewski, A., Howe, S. and Howe, T.: Project VALKYRIE: Laser-powered cryobots and other methods for penetrating deep ice on Ocean Worlds. Outer Solar System: Prospective Energy and Material Resources, 47-165, https://doi.org/10.1007/978-3-319-73845-1_4, 2018.

Takeuchi, N., Kohshima, S., and Segawa, T.: Effect of cryoconite and snow algal communities on surface albedo on maritime glaciers in south Alaska. Bulletin of Glaciological Research, 20, 21-27, 2003.

Taylor, G.T. and Sullivan, C.W.: Vitamin B12 and cobalt cycling among diatoms and bacteria in Antarctic sea ice microbial communities. Limnol. Oceanogr., 53, 1862-1877, https://doi.org/10.4319/lo.2008.53.5.1862, 2008.

Tedstone, A.J., Bamber, J.L., Cook, J.M., Williamson, C.J., Fettweis, X., Hodson, A.J., and Tranter, M.: Dark ice dynamics of the south-west Greenland Ice Sheet. The Cryosphere, 11, 2491-2506, https://doi.org/10.5194/tc-11-2491-2017, 2017.

van Beusekom, A.E., O'Nell, S.R., March, R.S., Sass, L.C., and Cox, L.H.: Re-analysis of Alaskan benchmark glacier mass-balance data using the index method (No. 2010-5247). US Geological Survey, https://pubs.usgs.gov/sir/2010/5247/pdf/sir20105247.pdf, 2010.

Yallop, M.L., Anesio, A.M., Perkins, R.G., Cook, J., Telling, J., Fagan, D., MacFarlane, J., Stibal, M., Barker, G., Bellas, C., and Hodson, A.: Photophysiology and albedo-changing potential of the ice algal community on the surface of the Greenland ice sheet. ISME J., 6, 2302-2313, http://dx.doi.org/10.1038/ismej.2012.107, 2012.

Zawierucha, K., Kolicka, M., Takeuchi, N., and Kaczmarek, Ł.: What animals can live in cryoconite holes? A faunal review. J. Zool. (Lond.), 295, 159-169, https://doi.org/10.1111/jzo.12195, 2015.

Zwally, H.J., Abdalati, W., Herring, T., Larson, K., Saba, J., and Steffen, K.: Surface melt-induced acceleration of Greenland ice-sheet flow. Science, 297, 218-222, https://doi.org/10.1126/science.1072708, 2002.

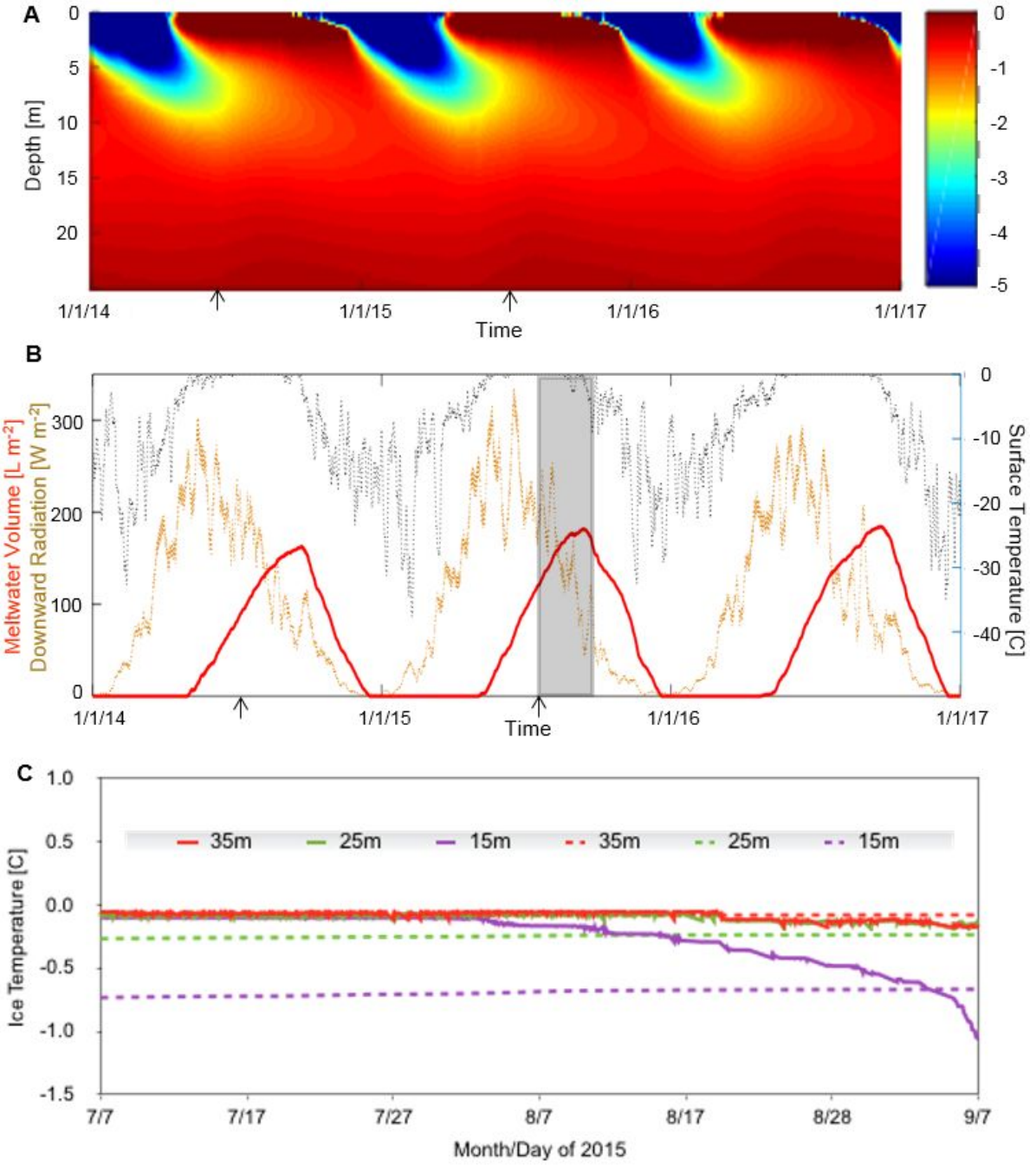

Figure 1. Temperature and ice water content during 2014 to 2016 (A) Modeled ice temperature was calculated using a finite difference solver to a one-dimensional diffusion-advection-production equation. Only values between 0 (red limit) and -5°C

(blue limit) are plotted. (B) The model is driven by the ERA-interim reanalysis 2 m-air temperature (black dots) and downward radiation data (brown dots) for the region (Dee et al., 2011). Both forcings are plotted at hourly intervals after smoothing with a daily (surface temperature) and weekly (radiation) running-average filter to suppress short-term variability. The greyed region in panel B represents the summer 2015 interval plotted in panel C when ice temperature data were collected. The arrows in panel A and B indicate the timing of the two field campaigns. (C) Comparison between ice temperatures observed with thermistors placed in a borehole at 15, 25, and 35 m below the surface from early July to early September of 2015 (solid lines) and the simulated ice temperatures (dashed lines) for the same depths below the surface of the model domain.

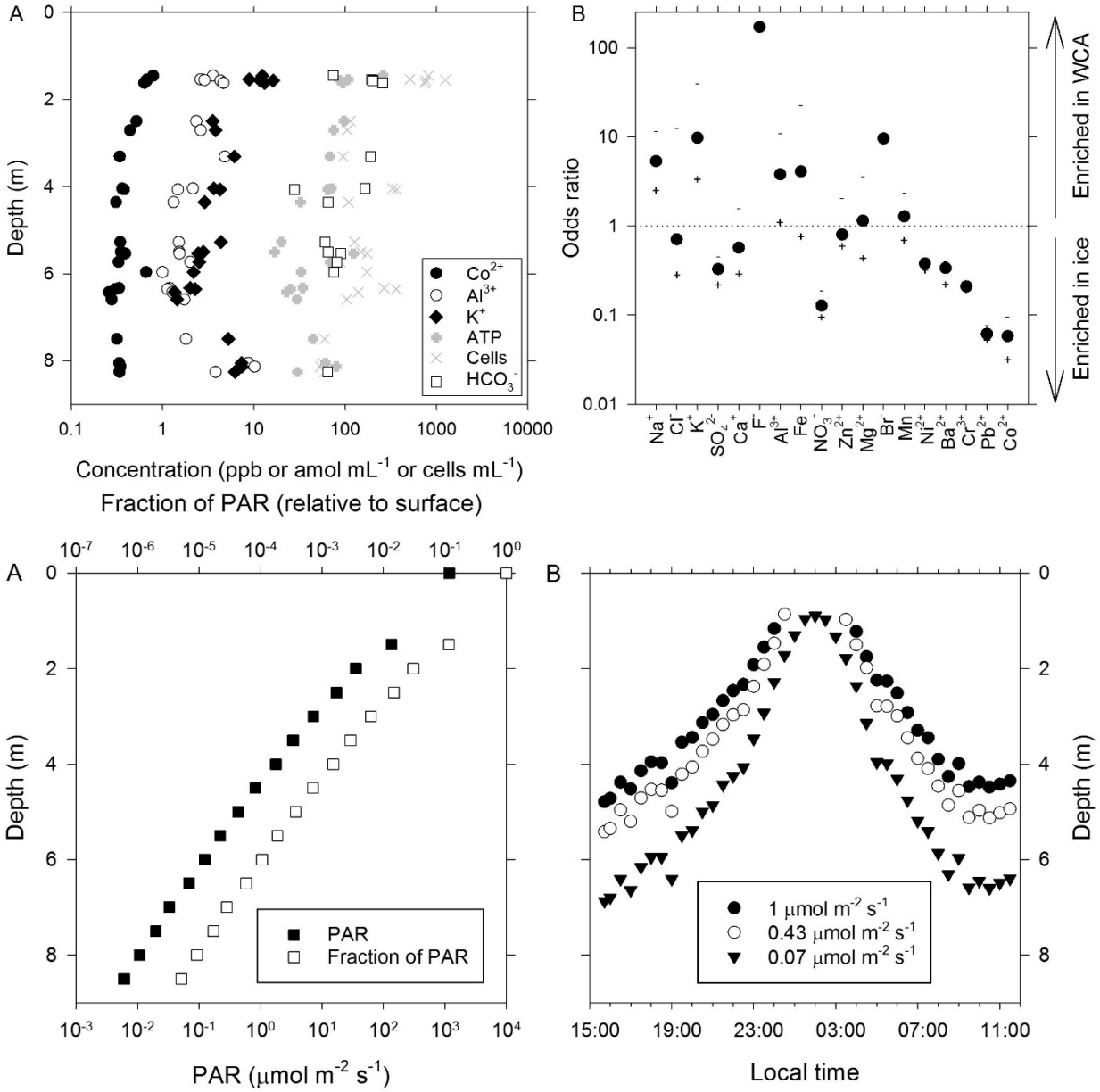

Figure 2. PAR optical properties of the near-surface ice during the 2014 ablation season. (A) Measurement of PAR attenuation to a depth of 8.5 m. (B) Diel pattern for select PAR fluxes that support oxygenic photosynthesis in cold and shaded aquatic environments (Priscu et al., 1988; Hawes and Schwarz, 2001). The data plotted were derived from an overnight measurement with the sensor at a depth of 3.5 m and then using data from (A) to extend the overnight profile to the upper 8.5 m ice column.

Figure 3. Geochemical composition of melted ice and water from the WCA. A) Depth profile for analytes correlated with the cell and/or ATP data. B) Ratio of compounds in the WCA water samples relative to the average in ice from depths of 1.4 to 11.3 m. The order of compounds is based on their abundance in the WCA sample (i.e., decreasing abundance from left to right). The plus and minus symbols are the ratios based on the maximum and minimum values, respectively, observed in the ice profile.

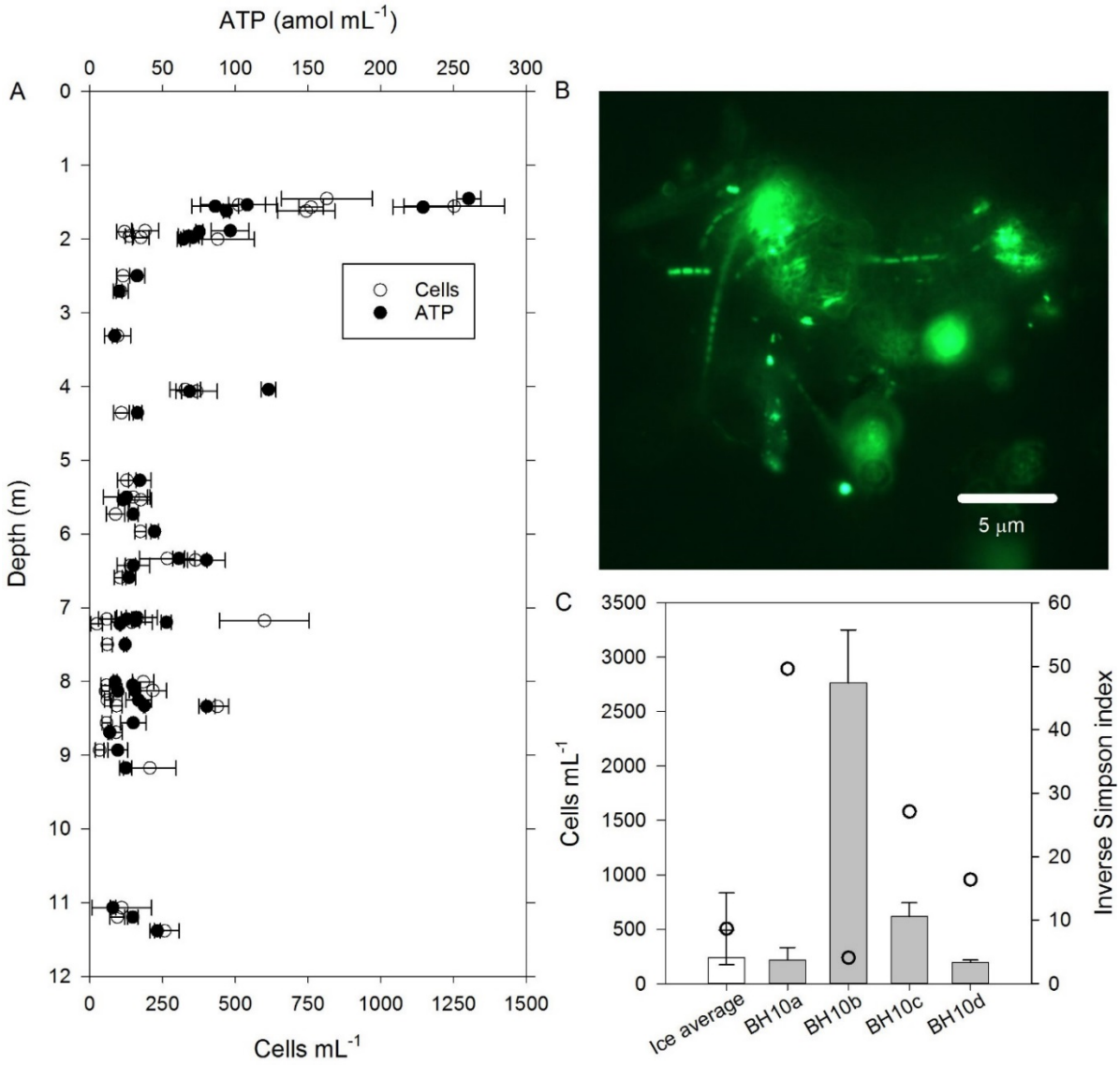

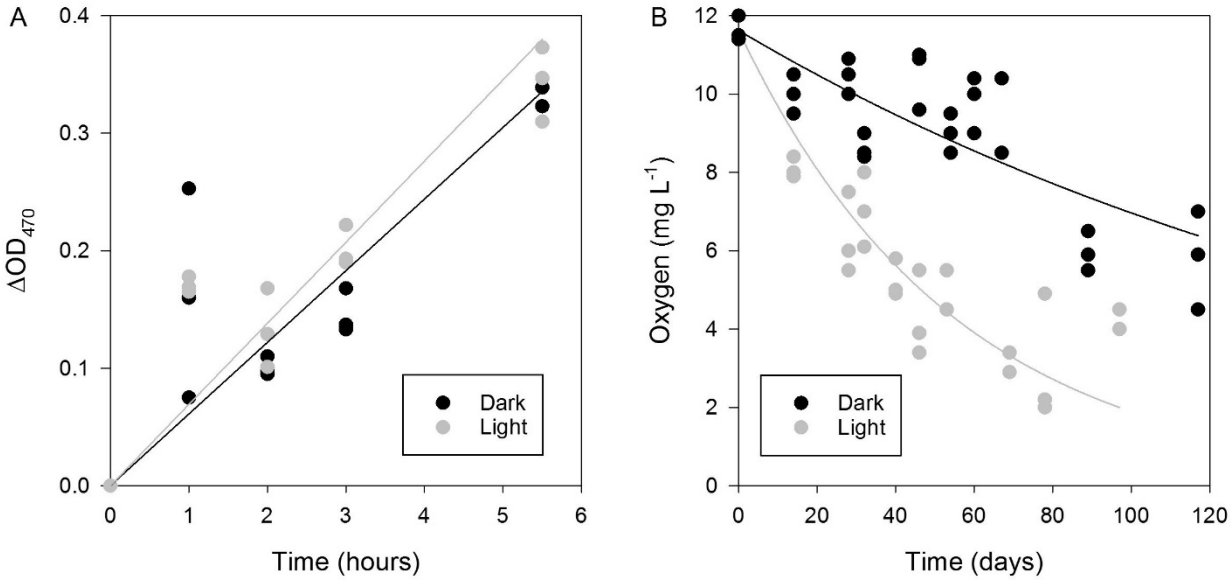

Figure 4. Cells and biomass in samples of melted ice and water from the WCA. A) Concentration of cells and ATP from depths of 1.4 to 11.3 m. B) Epifluorescent micrograph showing example of cell-particle aggregates observed in samples from the glacier's near-surface (sample BH4a). C) Comparison of community diversity (open circles) and cell concentration data from the ice (white bar) with water that percolated into the borehole (grey bars). The ice value was derived by averaging the data plotted in panel A. The inverse Simpson index for the ice is based on average values from sampled depths between 2 to 15 m (BH6a, BH6b, BH6c, BH7a, BH7b, and BH7c). The error bars in panels A and C indicate the standard deviation from the mean.

Figure 5. Respiratory activity of microorganisms in the WCA. (A) Time-dependent reduction of XTT for samples (BH5) incubated in situ. Linear regression models for the data are also plotted (B) Oxygen consumption in the light (~270 μmol photons m^2 s^{-1}) and dark over approximately 3 months at 5°C (sample BH10c). The data were fit with an exponential model (Dark, $y = 11.6e^{-0.00553}$, $r^2 = 0.676$; Light, $y = 11.6e^{-0.0167}$, $r^2 = 0.644$).

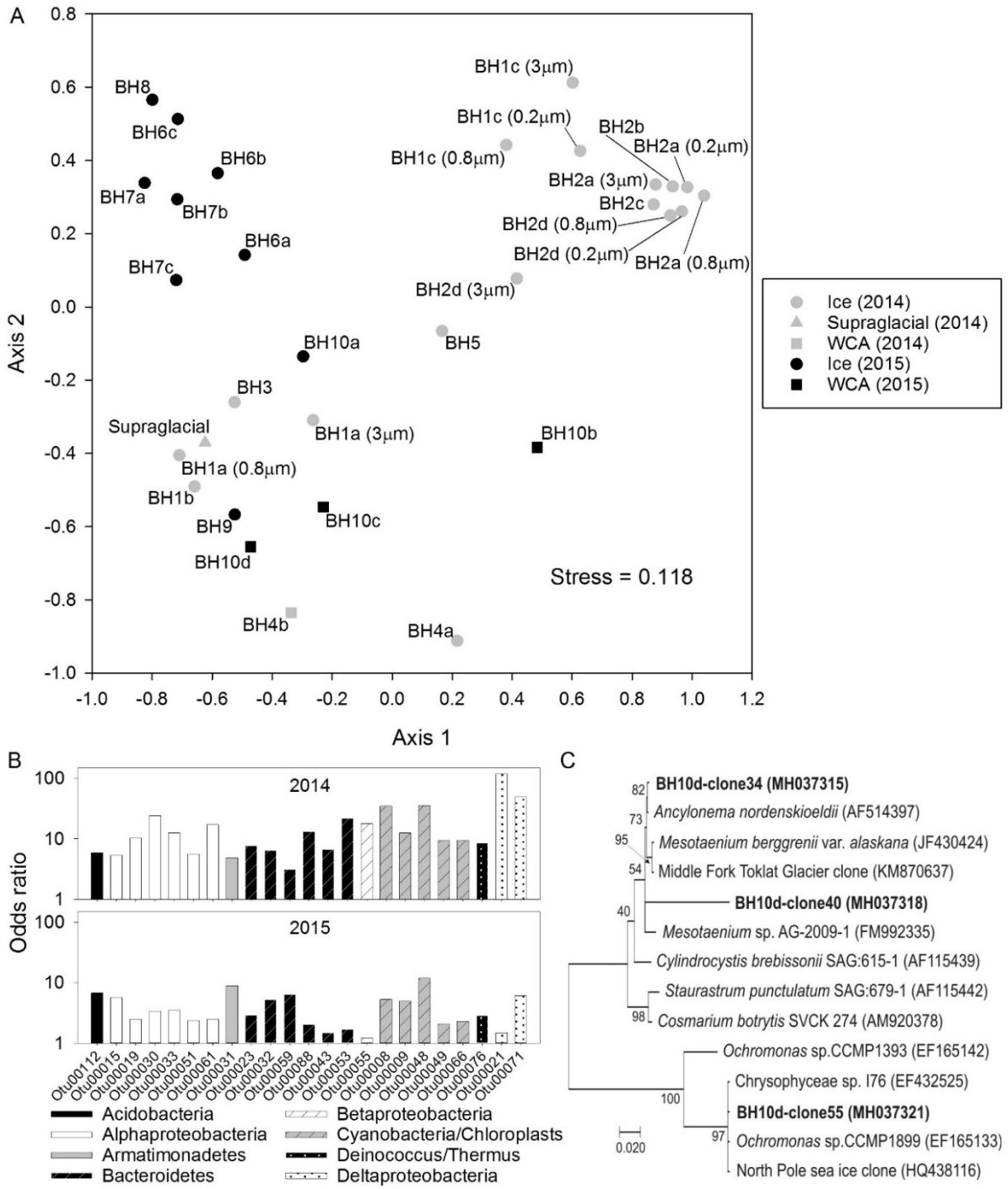

Figure 6. Microbial community structure in the ice and WCA based on analysis of 16S/18S rRNA genes. (A) NMDS

ordination plot of communities observed in samples of englacial (upper left and right) and near-surface (bottom) ice. (B) Odds ratios for taxa enriched in the near surface ice samples. The OTUs shown have abundances >0.25% of all sequences and odds ratios >5-fold in samples from 2014 or 2015. (C) Phylogenetic analysis of amplified 18S rRNA gene sequences (positions 566 to 1200, *Saccharomyces cerevisiae* numbering) related to algae in Zygnematophyceae and Chrysophyceae classes. Genbank accession numbers are listed in parentheses. The scale bar represents 0.020 substitutions per site and bootstrap values are shown as a percentage of 1000 replications.